Journal Pre-proof

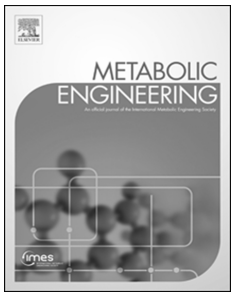

Reverse engineering of fatty acid-tolerant *Escherichia coli* identifies design strategies for robust microbial cell factories

Yingxi Chen, Erin E. Boggess, Efrain Rodriguez Ocasio, Aric Warner, Lucas Kerns, Victoria Drapal, Chloe Gossling, Wilma Ross, Richard L. Gourse, Zengyi Shao, Julie Dickerson, Thomas J. Mansell, Laura R. Jarboe

PII: S1096-7176(20)30083-5

DOI: https://doi.org/10.1016/j.ymben.2020.05.001

Reference: YMBEN 1672

To appear in: *Metabolic Engineering*

Received Date: 26 October 2019

Revised Date: 5 February 2020

Accepted Date: 2 May 2020

Please cite this article as: Chen, Y., Boggess, E.E., Ocasio, E.R., Warner, A., Kerns, L., Drapal, V., Gossling, C., Ross, W., Gourse, R.L., Shao, Z., Dickerson, J., Mansell, T.J., Jarboe, L.R., Reverse engineering of fatty acid-tolerant *Escherichia coli* identifies design strategies for robust microbial cell factories, *Metabolic Engineering* (2020), doi: https://doi.org/10.1016/j.ymben.2020.05.001.

Yingxi Chen: conceptualization, methodology, validation, formal analysis, investigation, resources, writing – original draft, review & editing; **Erin E. Boggess**: conceptualization, methodology, software, formal analysis, resources, data curation, writing – original draft, review & editing; **Efrain Rodriguez Ocasio**: conceptualization, methodology, formal analysis, investigation; **Aric Warner**: methodology, formal analysis, investigation, resources; **Lucas Kerns**: investigation, resources; **Victoria Drapal**: methodology, investigation, resources; **Chloe Gossling**: investigation, resources; **Wilma Ross**: conceptualization, methodology, software, validation, formal analysis, investigation, resources, writing – original draft, review & editing; **Richard L. Gourse**: conceptualization, methodology, writing – original draft, review & editing; **Zengyi Shao**: conceptualization, methodology, writing – original draft; **Julie Dickerson**: conceptualization, methodology, writing – original draft; **Thomas J. Mansell**: conceptualization, methodology, writing – original draft, review & editing; **Laura R. Jarboe**: conceptualization, methodology, writing – original draft, review & editing

Reverse engineering of fatty acid-tolerant *Escherichia coli* identifies design strategies for robust microbial cell factories

Yingxi Chen[1,2], Erin E. Boggess[3,4], Efrain Rodriguez Ocasio[5,6], Aric Warner[7], Lucas Kerns[1], Victoria Drapal[5,8], Chloe Gossling[1], Wilma Ross[9], Richard L. Gourse[9], Zengyi Shao[1,7], Julie Dickerson[3,4], Thomas J. Mansell[1,7*], Laura R. Jarboe[1,7*]

Author affiliations:

[1]Department of Chemical and Biological Engineering, Iowa State University, Ames, IA 50011

[2]Current location: Center for Synthetic Biology Engineering Research, Shenzhen Institutes of Advanced Technology, Chinese Academy of Sciences, Shenzhen 518055, China

[3]Department of Electrical and Computer Engineering, Iowa State University, Ames, IA 50011

[4]Bioinformatics & Computational Biology Graduate Program, Iowa State University, Ames, IA 50011

[5]NSF Center for Biorenewable Chemicals (CBiRC) Research Experience for Undergraduates, Ames, IA 50011

[6]Industrial Biotechnology Program, University of Puerto Rico Mayagüez, Puerto Rico, 00681

[7]Interdepartmental Microbiology Graduate Program, Iowa State University, Ames, IA 50011

[8]Department of Biological Systems Engineering, University of Nebraska-Lincoln, Lincoln, NE 68508

[9]Department of Bacteriology, University of Wisconsin-Madison, Madison, WI 53706

*co-corresponding authors

Corresponding authors:

Thomas J. Mansell, 4136 Biorenewables Research Laboratory, 617 Bissell Rd, Ames, IA 50011-1098, 515-294-7177, mansell@iastate.edu, ORCID iD 0000-0001-8807-4570

Laura R. Jarboe, 4134 Biorenewables Research Laboratory, 617 Bissell Rd, Ames, IA 50011-1098, 515-294-2319, ljarboe@iastate.edu, ORCID iD 0000-0002-4294-4347

Abstract

Adaptive laboratory evolution is often used to improve the performance of microbial cell factories. Reverse engineering of evolved strains enables learning and subsequent incorporation of novel design strategies via the design-build-test-learn cycle. Here, we reverse engineer a strain of *Escherichia coli* previously evolved for increased tolerance of octanoic acid (C8), an attractive biorenewable chemical, resulting in increased C8 production, increased butanol tolerance, and altered membrane properties. Here, evolution was determined to have occurred first through the restoration of WaaG activity, involved in the production of lipopolysaccharides, then an amino acid change in RpoC, a subunit of RNA polymerase, and finally mutation of the BasS-BasR two component system. All three mutations were required in order to reproduce the increased growth rate in the presence of 20 mM C8 and increased cell surface hydrophobicity; the WaaG and RpoC mutations both contributed to increased C8 titers, with the RpoC mutation appearing to be the major driver of this effect. Each of these mutations contributed to changes in the cell membrane. Increased membrane integrity and rigidity and decreased abundance of extracellular polymeric substances can be attributed to the restoration of WaaG. The increase in average lipid tail length can be attributed to the $RpoC^{H419P}$ mutation, which also confers tolerance to other industrially-relevant inhibitors, such as furfural, vanillin and n-butanol. The $RpoC^{H419P}$ mutation may impact binding or function of the stringent response alarmone ppGpp to RpoC site 1. Each of these mutations provides novel strategies for engineering microbial robustness, particularly at the level of the microbial cell membrane.

Keywords: evolution, membrane, stringent response, octanoic acid, reverse engineering , butanol

1. Introduction

Bioproduction of fuels and chemicals at the yields, rates and titers needed for economic viability is often impacted by toxicity of the product molecule to the microbial biocatalyst (Atsumi et al., 2010; Dunlop, 2011; Van Dien, 2013). One strategy for addressing this problem is to modify the production organism so that its sensitivity to the product molecule is decreased. Strategies for this modification commonly include rational strain engineering, often guided by -omics analysis (Foo et al., 2014; Jarboe et al., 2018; Jarboe et al., 2011; Lennen et al., 2011; Sandoval and Papoutsakis, 2016), adaptive evolution in the presence of the inhibitor (Chueca et al., 2018; Jin et al., 2016; Reyes et al., 2012; Royce et al., 2015), or screening of expression libraries (Sandoval et al., 2011; Zhang et al., 2012).

Rational strain development through the design-build-test-learn iterative cycle is effective, but requires a thorough understanding of the function of all of the relevant biological parts (Guan et al., 2016; Jarboe, 2018). Alternatively, the use of natural selection is not constrained by the existing body of knowledge. A variety of -omics tools can be used in the identification of mutations and reverse engineering of evolved strains, including whole-genome sequencing, transcriptome analysis, and fluxome analysis (Atsumi et al., 2010; Chueca et al., 2018; Foo et al., 2014). However, regardless of how mutations are identified, it is important that evolved strains displaying a desirable phenotype be subjected to reverse engineering so that these clever evolutionary strategies can be incorporated into the design of other strains. Ideally, this reverse engineering goes beyond identification of the mutation and confirmation that it contributes to the phenotype, and extends to understanding of how the mutation supports the evolved phenotype. As the cost of genome sequencing has decreased, the relative focus on identification of mutations and characterization of these mutations has shifted.

Here, we describe the reverse engineering of *E. coli* previously evolved for increased tolerance of octanoic acid (C8) in minimal medium, where this increased tolerance was associated with a five-fold increase in fatty acid production titers (Royce et al., 2015). Fatty acids are an attractive group of biorenewable chemicals with a large and increasing market and a wide range of applications (Desbois and Smith, 2010; Korstanje et al., 2015; Lopez-Ruiz and Davis, 2014; Tee et al., 2014). They also play a role in microbial pathogenesis (Nguyen et al., 2016). Short- and medium-chain fatty acids are well-characterized in terms of their damaging effects on the microbial cell membrane (Jarboe et al., 2018; Lennen et al., 2011; Liu et al., 2013; Sherkhanov et al., 2014). Therefore, design strategies that are learned from strains evolved for increased tolerance of these fatty acids may be applicable to engineering tolerance of other membrane-damaging compounds, such as n-butanol (Fletcher et al., 2016; Reyes et al., 2012). Here, we characterize the impact of mutations acquired during evolution for their impact on increased fatty acid production and alterations in properties of the microbial cell membrane. Each of the mutations acquired by the evolved strains were found to contribute to the evolved phenotype. A mutation within RNA polymerase was also found to increase tolerance to other membrane-damaging bio-products.

2. Materials and Methods

Full materials and methods are provided with the Supplemental Data and are briefly summarized here.

2.1 Whole-genome sequencing and verification of mutations

The Illumina Genome Analyzer II platform for high throughput sequencing was used for whole genome sequencing at the Iowa State University DNA facility, using software and

algorithms as previously described to identify mutations (Royce et al., 2013a). All mutations were verified by Sanger sequencing.

2.2 Assessment of inhibitor tolerance and nutrient downshift

Overnight seed cultures were inoculated into 250 mL baffled flasks with 25 mL MOPS with 2.0 wt% dextrose and the relevant inhibitor. Unless stated otherwise, growth was performed at 37°C and 200 rpm and the media pH was adjusted to 7.00±0.05. Other inhibitors were added to the following concentrations: 10 mM hexanoic acid (C6); 600 mM NaCl; 65.6 mM levulinic acid; 200 mM citrate; 54.3 mM sodium formate; 11.9 mM hydroxybenzoate; 3.6 mM trans-ferulic acid; 0.6% v/v n-butanol; 0.6% v/v iso-butanol; 2% v/v ethanol; 200 mM succinate; 6.6 mM vanillin; 10.4 mM furfural; 9.3% w/v glucose. Nutritional downshift was performed as previously described (Ross et al., 2013). Briefly, cells were grown to OD 0.6 – 0.8 in LB, washed in MOPS minimal medium, and resuspended in either fresh LB or MOPS minimal medium.

2.3 Fatty acid production

Strains transformed with the pJMY-EEI82564 plasmid encoding the TE10 thioesterase were grown on LB plates with ampicillin and incubated at 30°C overnight. Individual colonies were cultured in 250 mL flasks in 10 mL LB with ampicillin at 30°C on a rotary shaker at 250 rpm overnight. Seed cultures were inoculated at an approximate OD_{550} of 0.1 into 250 mL baffled flasks containing 50 mL of LB with 1.5 wt% dextrose, ampicillin, and 1.0 mM isopropyl-β-D-thiogalactopyranoside (IPTG). The flasks were incubated in a rotary shaker at 250 rpm and 30°C.

Fatty acids were extracted and further derivatized from samples containing both media and cells. The fatty acid methyl esters (FAMEs) were measured with an Agilent 6890 Gas

Chromatograph coupled to an Agilent 5973 Mass Spectrometer (GC-MS) at the ISU W.M. Keck Metabolomics Research Laboratory.

2.4 Extracellular polymeric substance (EPS) extraction and quantification

The total extracellular protein and polysaccharide were determined as previously described (Liang et al., 2016). Briefly, cells were grown on LB agar plates overnight, suspended in 0.85 wt% NaCl solution and quantified. The cell suspension was centrifuged at 16,300×g, at 4°C for 30 min, the supernatant was passed through a 0.45 µm filter and 90 mL of ice-cold 100% ethanol was added. The mixture was incubated at -20°C for 24 h. Then, the EPS pellet was harvested by centrifuging at 16,300×g for 30 min at 4°C, drying at room temperature and resuspension in 20 mL DI water.

2.5 Membrane characterization

Cells were grown to mig-log phase (OD_{550}≈1) in 25 mL of MOPS 2.0 wt% dextrose in 250 mL flasks with shaking at 37°C and 250 rpm and harvested by centrifugation at 4,500×g and room temperature for 10 min. Cells were washed twice with PBS pH 7.00±0.05 and resuspended to OD_{550}~1 in PBS containing 10 mM octanoic acid at pH 7.0 and then incubated at 37°C for 1 hour. For characterization of membrane permeability, the cell suspension was stained with SYTOX Green (Invitrogen, Carlsbad, CA) (Roth et al., 1997). Measurement of DPH polarization used 1,6-diphenyl-1, 3, 5-hexatirene (DPH, Life Technologies, Carlsbad, CA, USA) (Royce et al., 2013b). Measurement of cell surface hydrophobicity was performed as previously described (Rosenberg et al., 1980).

For measurement of membrane lipid composition, cells were grown to mid-log, harvested and resuspended in MOPS 2.0 wt% dextrose with or without 30 mM octanoic acid at pH 7.0, and

incubated for 3 hours at 37°C. Cells were harvested and processed to recover the fatty acids, which were then derivatized and measured by GC-MS.

3. Results

3.1 Identification and timing of mutations

Evolved strains LAR1 and LAR2 were previously isolated as distinct single colonies from the same liquid culture after seventeen serial dilutions in the presence of exogenous C8 at neutral pH in defined growth medium (Royce et al., 2015). Parent strain ML115 was previously engineered from the K-12 strain MG1655 to inactivate fatty acid beta-oxidation and acetate production via deletion of *fadD, poxB* and *ackA-pta* (Li et al., 2012). Mutations in LAR1 and LAR2 relative to ML115 were determined via Illumina sequencing, alignment to MG1655 as the reference genome, and verified by Sanger sequencing (Table 1). Alignment of parent strain ML115 to the reference genome revealed the presence of a 768-bp insertion sequence within lipopolysaccharide (LPS) glucosyltransferase I (WaaG). As discussed below, it seems that this mutation was implemented unintentionally during the development of ML115. LAR1 and LAR2 both have restored function of WaaG and a single amino acid change within the β' subunit of RNA polymerase RpoC, and each has a unique mutation in the BasS-BasR two-component signal transduction system. The shared *waaG* and *rpoC* mutations are most likely due to the fact that these strains share a common ancestor.

The order and timing of these mutations were determined by PCR and restriction digestion of samples taken periodically during the sequential transfers (Figure S1). The restoration of *waaG* occurred first, and relatively quickly, with only the ML115 version of *waaG* being observed at the end of the second transfer and only the restored version of *waaG* ($waaG^R$) being observed at the end of the third transfer. During these transfers, C8 was being supplied at a

concentration of 10 mM. By the thirteenth transfer, the concentration of exogenous C8 had been increased to 30 mM, and the single base pair mutation in *rpoC* was present in all cells. The mutations in *basS* and *basR* in strains LAR2 and LAR1, respectively, occurred after the fifteenth transfer, at which time 30 mM C8 was still being used as the selective pressure.

WaaG adds the first glucose of the outer core of LPS (Yethon et al., 2000). The mutation acquired by the evolved strains within *waaG* resulted in a restoration of the wild-type MG1655 sequence. The insertion sequence in *waaG* in ML115 not only abolished WaaG function, but also likely altered the expression of downstream genes *waaPSBOJ*. The deletion of *waaG* has previously been reported to result in a truncated LPS core and loss of flagella and pili (Parker et al., 1992) as well as altered cell surface hydrophobicity, outer membrane permeability, and biofilm formation (Wang et al., 2015).

The single base pair mutation from adenine to cystosine at position 1256 in *rpoC* results in the amino acid substitution from proline to histidine at position 419 in the RpoC protein. This mutation was reported, though not characterized, in our previous publication (Royce et al., 2015) and was also detected in strains evolved for tolerance of octanoic acid and glutaric acid (Lennen et al., 2018; Lennen et al., 2019). The close proximity of the H419P substitution to ppGpp binding site 1 in RNA polymerase (Ross et al., 2016) (Figure 1) is striking, and the effect of a proline substitution at position 419 could be expected to alter the conformation and function of this binding site. The stringent response alarmone ppGpp binds to two sites in *E. coli* RNA polymerase (site 1 and site 2) and alters transcription from a large number of promoters during the stringent response to stress conditions. Site 1 has been previously characterized biochemically, genetically, and structurally (Ross et al., 2016; Ross et al., 2013; Zuo et al., 2013), and contributes to the stringent response (Ross et al., 2016; Sanchez-Vazquez et al.,

2019). Residues in both RpoC (including R417) and the adjacent RpoZ (omega) subunit participate in ppGpp binding to site 1 and are required for its effects on transcription. These residues span the junction between two mobile modules of RNA polymerase (core and shelf), and ppGpp binding has been proposed to restrict the relative motion of the modules, thereby affecting transcription (Ross et al., 2013; Zuo et al., 2013).

The two evolved strains contain different mutations within the BasS-BasR two-component regulatory system. LAR1 has a single amino acid change, from aspartic acid to tyrosine, within the response regulator receiver domain of BasR. LAR2 has an in-frame deletion of nine amino acids from the histidine kinase domain of BasS. The BasS-BasR two-component system senses and responds to changes in environmental conditions related to metals (Ogasawara et al., 2012).

3.2 All three mutations are required for LAR1-level C8 tolerance

It has been previously demonstrated that evolved strain LAR1 has significantly increased tolerance to exogenously supplied fatty acids relative to its parent strain, ML115 (Royce et al., 2015). To determine the contribution of each mutation to C8 tolerance, we systematically re-constructed the LAR1 mutations in parent strain ML115 and investigated the *basS* mutation from LAR2 (strains YC001-011, Table 2). When the mutations were implemented in the order in which they occurred, sequentia restoration of the evolved phenotype was observed.

In the presence of 10 mM exogenous C8, the parent strain showed a four-fold lower specific growth rate ($p \leq 0.0038$) and 10-fold lower 24 hr OD relative to LAR1. Restoration of WaaG ($waaG^{R}$) (strain YC001) more than doubled the specific growth rate and final OD, though both metrics were still significantly lower than LAR1. Replacement of *rpoC* with $rpoC^{H419P}$ in the parent strain with restored WaaG (strain YC005) resulted in a growth rate and final OD that

were statistically indistinguishable from LAR1. Thus, this characterization in the presence of 10 mM C8 gives the initial impression that the evolved strain phenotype can be completely attributed to *waaG*^{R} and *rpoC*^{H419P} and that the *basR* mutation is not required. However, further characterization showed that all three mutations (strain YC010) were required for reproduction of the evolved strain growth rate in the presence of 20 mM C8. Specifically, the parent strain with only *waaG*^{R} and *rpoC*^{H419P}, but still encoding the wild-type *basR* (YC005), had a significantly lower growth rate relative to LAR1. Upon replacement of the genomic wild-type *basR* with *basR** to generate strain YC010, the specific growth rate in the presence of 20 mM exogenous C8 was statistically indistinguishable from the evolved strain.

Characterization of the individual mutations in the presence of 10 mM C8 also provided insight into their role in the evolved phenotype. As described above, restoration of WaaG resulted in an increase in specific growth rate and final OD relative to ML115, but still significantly lower than LAR1. Implementation of only the *rpoC*^{H419P} mutation (strain YC003) did significantly increase the specific growth rate relative to ML115 in the absence of C8, but did not impact the growth rate during C8 challenge or the 24-hr OD in either condition. Implementation of only the *basR** (YC003) or *basS** (YC004) mutation resulted in no significant difference relative to parent strain ML115 in the presence of 10 mM C8.

Implementation of these mutations also resulted in significant changes in specific growth rate and 24-hr OD_{550} even in the absence of C8 (Table 2). Specifically, implementation of *rpoC*^{H419P} in ML115 (strain YC002) significantly increased the growth rate relative to both ML115 and LAR1. Also, implementation of *waaG*^{R} and *basS** or *basR** without also conferring the *rpoC*^{H419P} mutation (strains YC006 and YC007) resulted in a decrease in the specific growth rate relative to both ML115 and LAR1.

These results demonstrate that the order of combination of mutations is important for assessing their contribution to the evolved phenotype and that each of the three general mutations acquired during evolution contribute to the evolved phenotype.

3.3 WaaG^{R} and RpoC^{H419P} are sufficient for LAR1-level fatty acid production

The characterization of growth in the presence of exogenous C8 demonstrates that restoration of WaaG function, the single amino acid change in RpoC^{H419P}, and alteration of the BasS-BasR two-component regulatory system all contribute to the increased C8 tolerance of LAR1. However, since the goal of increasing C8 tolerance is to increase fatty acid production, we also assessed the impact on fatty acid production in rich media (Figure 2A). Fatty acid production was enabled via the expression of the *Anaerococcus tetradius* thioesterase (TE10), which primarily produces octanoic acid (Jing et al., 2011).

While restoration of WaaG^{R} increased fatty acid titers, a much more dramatic increase was observed when combined with the RpoC^{H419P} mutation. Specifically, while the parent strain only produced 80 mg/L of fatty acids over 72 hrs, restoration of WaaG^{R} increased that value more than 2-fold to 188 mg/L ($p = 0.004$), and subsequent replacement of the wild-type RpoC with RpoC^{H419P} (YC005) further increased the titer to 780 mg/L (approximately 5 mM), a nearly 10-fold increase relative to the parent, comparable to the 783 mg/L produced by evolved strain LAR1. Consistently, the addition of BasR* to ML115+*waaG*^{R}+*rpoC*^{H419P} (YC010) did not further increase the production titers (*data not shown*). The lack of impact observed for the BasR* mutation is similar to the growth rate characterization (Table 2), in that the effect of BasR* was apparent only in the presence of 20 mM exogenous C8, but not 10 mM C8. The dramatic increase in fatty acid titer for strain YC005 relative to YC001 demonstrates the impact of the *rpoC*^{H419P} mutation on fatty acid production.

These differences in fatty acid titer cannot be solely attributed to growth of the production strain. For example, restoration of *waaG*^{R} resulted in a 4-fold increase in OD_{550} during fatty acid production relative to the parent, but the fatty acid titers only increased by slightly more than 2-fold (Figure 2B). In contrast, there was no significant difference in the OD of the ML115+*waaG*^{R} and ML115+*waaG*^{R}+*rpoC*^{H419P} strains over the course of fatty acid production, despite a 4-fold difference in fatty acid titers.

3.4 Each mutation contributes to membrane changes

The cell membrane plays a vital role in microbial tolerance, particularly in the production of biorenewable fuels and chemicals (Jarboe et al., 2018; Lennen and Pfleger, 2013; Luo et al., 2009; Qi et al., 2019; Sherkhanov et al., 2014; Tan et al., 2017; Tan et al., 2016). It is also known that the cell membrane is vulnerable to damage by short- and medium-chain fatty acids (Lennen et al., 2011; Royce et al., 2013b; Royce et al., 2015) and other appealing bio-products (Lian et al., 2016). Our previous characterization of LAR1 and ML115 demonstrated alteration of the cell membrane in terms of integrity, fluidity, and lipid tail distribution (Royce et al., 2015). Thus, in addition to identifying which mutations contribute to increased C8 tolerance and increased fatty acid production, here we also assessed their contribution to these altered membrane properties (Figure 3).

Evolved strain LAR1 showed drastically increased membrane integrity during exogenous C8 challenge relative to parent strain ML115, as evidenced by a decrease in permeability to the SYTOX nucleic acid dye (Figure 3A), as previously reported (Royce et al., 2015). Characterization of single and combined mutants demonstrates that restoration of WaaG, the first mutation acquired during adaptive laboratory evolution, is responsible for the increased membrane integrity of LAR1. This is consistent with previous reports that deletion of *waaG* in *E.*

coli decreased outer membrane integrity (Wang et al., 2015). Implementation of only the *rpoC*^{H419P} mutation in ML115 (YC002) did not increase membrane integrity, but implementation of only the *basS** or *basR** mutations did, though not to the level observed for only *waaG*^{R}. Thus, the first mutation that occurred during evolution of LAR1 corrected the problematic loss of membrane integrity in the presence of exogenous C8. In strains YC003 and YC004, mutation of the BasS-BasR system also impacts membrane integrity, but this effect is only observed in the absence of a functional WaaG.

For appropriate function, the membrane should be neither too fluid nor too rigid. It has been previously demonstrated that exogenous C8 increases membrane fluidity (Royce et al., 2013b) and that engineered strains with increased membrane rigidity have an increase in C8 tolerance and production (Tan et al., 2016). Previous characterization of LAR1 showed significantly lower membrane fluidity, and thus higher membrane rigidity, than the parent strain (Royce et al., 2015), as evidenced by higher 1,6-diphenyl-hexa-1,3,5-triene (DPH) polarization values. Here, characterization of single and combined implementation of our mutations showed that, as with the alteration of membrane permeability, the restoration of WaaG functionality is sufficient to account for the difference in ML115 and LAR1 rigidity (Figure 3B).

Changes in the relative distribution of the various membrane lipids in stressful conditions have been widely reported (Liu et al., 2013; Royce et al., 2013b; Venkataramanan et al., 2014) and targeted changes to this distribution have been found to be effective in improving tolerance and sometimes improving production (Jarboe et al., 2018; Lennen and Pfleger, 2013; Luo et al., 2009; Sandoval and Papoutsakis, 2016; Sherkhanov et al., 2014). We have previously described the altered membrane lipid distribution of LAR1 relative to ML115, with the conclusion that the average lipid length was consistently higher in LAR1 across a range of conditions (Royce et al.,

2015). Thus, the membrane lipid distribution for the various strains characterized here is presented in terms of average lipid length. Characterization of the single and combined mutants showed that restoration of functional WaaG (YC001) contributed to, but did not fully account for, the increase in average lipid length. However, expression of RpoC^{H419P} in parent strain ML115, either as the only implemented mutation (YC002) or in conjunction with *waaG*^{R} (YC005) or with *waaG*^{R} and *basR** (YC010), fully accounted for the increase in average lipid length (Figure 3C).

A loss of membrane integrity and perturbation of the membrane fluidity indicate problems with the membrane function. Contrastingly, cell surface hydrophobicity can range widely without any apparent detrimental impact on cell health (Liang et al., 2016). While the membrane composition, in terms of phospholipid heads, lipid tails and proteins, is a substantial driver of membrane integrity and fluidity, hydrophobicity is influenced by various other proteins and sugars (Liao et al., 2015). We have previously observed that increased cell surface hydrophobicity is associated with increased fatty acid production by *E. coli* (Chen et al., 2018). Here we report that evolved strain LAR1 also differs from parent strain ML115 in that is has a substantially larger cell surface hydrophobicity (Figure 3D).

Reproduction of this increase in cell surface hydrophobicity requires the combined implementation of *waaG*^{R}, *rpoC*^{H419P} and *basR** (YC010). When only the *waaG*^{R} mutation was expressed in ML115, there was no change in hydrophobicity (Figure 3D). Expression of only *rpoC*^{H419P}, *basR** or *basS** in ML115 also did not reproduce the evolved strain value, but combination of *waaG*^{R} and *rpoC*^{H419P} (YC005) resulted in a hydrophobicity value higher than the value observed for any of the single mutants. The presence of all three mutations, *waaG*^{R}, *rpoC*^{H419P} and *basR**, reproduced the evolved strain value.

These results demonstrate that each of the mutations identified in LAR1 contributes to at least one of the alterations in membrane properties.

3.5 Restoration of WaaG^R dramatically impacts EPS sugar production

Since *waaG* encodes lipopolysaccharide (LPS) glucosyltransferase I, which adds the first glucose of the outer core of LPS (Yethon et al., 2000), we sought to determine the overall effect on extracellular polymeric substances (EPS). Restoration of *waaG* (*waaG^R*) decreased the production of the two major EPS, polysaccharides and proteins. Parent strain ML115, which encodes the disrupted form of *waaG*, produced approximately 2.8 µg EPS polysaccharides per 10^8 cells (Figure 4A), which is nearly an order of magnitude higher than the approximately 0.3 µg per 10^8 cells previously observed for a set of 77 environmental *E. coli* isolates (Liang et al., 2016). Restoration of WaaG via gene replacement with *waaG^R* in ML115 (YC001) resulted in a more than 10-fold decrease in EPS sugar production (Figure 4A).

It is expected that parent strain ML115, encoding only the disrupted form of *waaG*, should only be able to produce the inner core of LPS while strains encoding the restored *waaG^R* gene should produce complete LPS (Ren et al., 2016). The colony morphology of ML115, LAR1, and ML115+*waaG*^{R} (YC001) clearly differ (Figure 4B). Previous characterization of a *waaGPBI* deletion mutant described a mucoid colony morphology (Parker et al., 1992), consistent with our observations for ML115 (Figure 4B), but not for LAR1 and ML115+*waaG^R* (Figure 4B). The deletion of *waaG* has previously been reported to result in a truncated LPS core and loss of flagella (Parker et al., 1992). This is consistent with TEM imaging of our strains, in that flagella are visible for LAR1 but not for ML115 (Figure 4C).

3.6 RpoC^{H419P} impacts tolerance of other inhibitors and possibly the stringent response

As part of the global transcription machinery, RpoC is involved in all transcription events. Replacing RpoC with RpoC^{H419P} in ML115 (YC002), without implementation of any other mutations, was observed to significantly increase the specific growth rate both in our control condition and in the presence of 10 mM exogenous C8 (Table 2), to increase the average membrane lipid length (Figure 3C) and increase the cell surface hydrophobicity (Figure 3D). To gain further insight into the applicability of this mutation to other bio-production scenarios, we compared the growth of ML115 expressing the restored form of WaaG (YC001) to ML115 expressing WaaG^{R} and RpoC^{H419P} (YC005) in the presence of a variety of inhibitors (Figure 5A). These experiments were done in the presence of the restored form of *waaG* (*waaG*^{R}) in order to increase similarity to other *E. coli* strains.

The presence of RpoC^{H419P} relative to wild-type RpoC was observed to increase the specific growth rate by more than 25% in the presence of furfural, vanillin, octanoic acid (C8), hexanoic acid, n-butanol and citrate (Figure 5A). Growth rates in the presence of moderate thermal stress (42°C) and low pH (5.5) were observed to decrease by more than 25% (Figure 5A). Thus, the RpoC^{H419P} mutation confers a growth benefit in the presence of many, but not all, inhibitory molecules and conditions.

The decrease in thermotolerance is especially intriguing, given the previous reported association of thermotolerance and the stringent response, as mediated by the alarmone ppGpp. Specifically, ppGpp has been shown to accumulate following heat shock (Abranches et al., 2009) and strains deficient in ppGpp production have increased sensitivity to heat shock (Yang and Ishiguro, 2003). The mutated residue in RpoC^{H419P} is very close to residue 417, which has been reported to be a component of the site 1 binding site for ppGpp on the RNA polymerase complex

(Ross et al., 2016; Ross et al., 2013). Visualization of H419 within the existing structural model (Zuo et al., 2013) indicates that this amino acid does not directly contact ppGpp or interact directly with the active site (Figure 1). However, proline substitutions can be disruptive to local structure, and this one could potentially alter the conformation of residues directly contacting ppGpp, thereby altering binding or function of ppGpp indirectly.

Modifications to the RNA polymerase complex that eliminate site 1 (RpoC R362A, R417A, K615A and RpoZ Δ2-5) have been previously described (Ross et al., 2016). Characterization here of this site 1 null mutant and the corresponding control (RLG 14535) supports the possible role of site 1 in C8 tolerance. Specifically, the site 1 null mutant had increased tolerance to C8, isobutanol and n-butanol, as evidenced by an increase in the specific growth rate (Figure 5B). However, the magnitude of the increase in growth rate in the presence of C8 or n-butanol relative to the corresponding control was not as large for the site 1 mutant as was observed with $RpoC^{H419P}$ ($p < 0.001$).

The site 1 mutant was previously demonstrated to have delayed recovery from a nutrient downshift from rich medium to minimal medium relative to the corresponding wild-type control (Ross et al., 2016). Specifically, the wild-type control strain had a lag time of approximately 3 hours, while the site 1 mutant had a lag time of approximately 6 hours (Ross et al., 2016). Here, we observed that the strain expressing the H419P mutation (YC005) did not show this delayed recovery from a similar nutrient downshift relative to the wild-type control (YC001), with both strains having a lag time of approximately 5.5 hours (Figure 5C).

These results suggest that the H419P mutation may affect binding or function of ppGpp at site 1, but may also have features distinct from previously-characterized mutations. It is possible that both the differing magnitude of the growth rate changes and the differing recovery

from nutrient downshift are due to other genetic differences in the strain with the H419P mutation and the strain with the characterized ppGpp Site 1 mutations (e.g., *fadD*, *poxB*, *ackA-pta*). However the RpoC^{H419P} mutation is an intriguing strategy for possibly increasing production of other bio-products beyond C8.

4. Discussion

Here, we demonstrate a framework for characterization of evolved strains, with identification of genetic modification strategies that may be applicable to improved microbial performance in other conditions. Not only did we confirm that each of the known mutations contribute to the phenotype of the evolved strain, we were also able to demonstrate the impact of individual mutations on cell physiology (Figure 6). The restriction analysis used here to assess the timing of the mutations would not have detected other mutations within the heterogenous population. However, the demonstration that the three mutations characterized here are sufficient for recreation of the evolved strain phenotype indicates that all of the important mutations were identified. This also demonstrates that evolutionary studies involving only a small number of evolved genomes are still capable of contributing to the design, build, test and learn metabolic engineering design cycle.

Restoration of WaaG increased membrane integrity and increased the membrane rigidity, as evidenced by DPH polarization. This finding emphasizes the potential of cell-surface sugars and proteins as targets for engineering membrane properties and microbial robustness, consistent with previous reports using a modified version of carbon storage regulator A (CsrA) to modulate the abundance of these sugars and proteins (Jin et al., 2017). Mutations within the BasS-BasR system contribute to the increased tolerance of high C8 concentrations and also to the change in cell surface hydrophobicity. The BasS-BasR system has been previously recognized as

contributing to tolerance of n-butanol (Reyes et al., 2012), and this work provides further support for utilizing this system as an engineering target.

The mutation within RpoC^{H419P} is able to fully account for the increase in average lipid length observed in LAR1, contributes to the increase in cell surface hydrophobicity, and when expressed in conjunction with the restored WaaG resulted in a dramatic increase in C8 production titers. This mutation also increased tolerance to a variety of other inhibitors that are relevant to economically viable bio-production, such as furfural, vanillin, and n-butanol. Comparison of the RpoC^{H419P} mutation to a mutation in one of the ppGpp-RpoC binding sites (site 1) shows that while the magnitude of the impact is higher for RpoC^{H419P}, the two mutations both conferred increased growth rate in the presence of exogenous C8. The increased heat sensitivity conferred by RpoC^{H419P} and the increase in specific growth rate in the absence of C8 challenge are also consistent with perturbed sensitivity of RNA polymerase to ppGpp (Table 2). Thus, the interaction of the stringent response alarmone ppGpp and RNA polymerase appears to be relevant to tolerance and production of short- and medium-chain fatty acids.

Other reports of strain evolution have presented mutations within the stringent response system as a clever strategy for increasing tolerance to biorenewable fuels and chemicals. For example, evolution of *E. coli* for tolerance to n-butanol, isopropanol, ethanol and 2,3-butandiol each found mutations within ppGpp synthetase I, encoded by RelA (Horinouchi et al., 2017; Horinouchi et al., 2015; Lennen et al., 2019; Reyes et al., 2012). Alcohols have been reported to interact with translation machinery (Laughrea et al., 1984; So and Davie, 1964) and stimulate production of ppGpp (Mitchell and Lucaslenard, 1980). Up to a quarter of the cell's promoters have been shown to be affected by the stringent response (Sanchez-Vazquez et al., 2019). All of the 10 genes classified as involved in fatty acid biosynthesis initiation and elongation of

saturated fatty acids showed a statistically significant decrease in transcript abundance 5 minutes after induction of *relA* in a strain expressing wild-type RNA polymerase (Sanchez-Vazquez et al., 2019). However, in an isogenic strain expressing RNA polymerase lacking both of the ppGpp binding sites, only one of these 10 genes showed a statistically significant perturbation in expression following *relA* induction (Table S4). It is possible that, like alcohols, short-chain fatty acids interact with translation machinery. Relaxing of the stringent response, such as by a mutation within RpoC, seems to contribute to the increased growth and fatty acid titers observed in evolved strain LAR1 and reconstructed evolved strain YC005.

It is possible that the original insertion that disrupted the *waaG* gene occurred unintentionally during the creation of ML115 from MG1655. ML115 is a triple knockout strain engineered to improve fatty acid titer by inactivation of acetate production and the β-oxidation pathway (Li et al., 2012). These gene deletions were implemented by λ Red recombineering and P1 phage transduction, methods that require multiple electroporation, plasmid curing, and phage infection steps, especially in an automated framework. As these processes are often lethal to a large portion of the cells, it may be that a change in membrane composition via the incorporation of an insertion element made a sub-population more robust to these challenges, which was then enriched during subsequent steps. The drastic change in cell properties conveyed by the *waaG* insertion should serve as a cautionary note to those who perform multiple transformation or transduction steps. However, mutations to *waaG* and its pathway are easily identifiable by mucoid colony phenotype (Figure 4B), consistent with an increase in EPS (Figure 4A). Mucoid colonies can often be present following P1 transduction (Thomason et al., 2014) and previous studies have shown that mucoid phenotypes decrease transduction efficiency (Zhang et al., 2008)

and that mutations via spontaneous insertion of transposable elements often arise during these procedures (Nagahama et al., 2006).

The microbial cell membrane is a frequently-recognized engineering target when addressing microbial robustness, and here we have characterized several strategies for membrane engineering. These results also contribute to the growing body of evidence that the stringent response plays a substantial role in improving not just tolerance, but also production, of fuels and chemicals at economically viable titers.

5. Acknowledgments

This work was supported by the National Science Foundation (NSF) Engineering Research Center for Biorenewable Chemicals (CBiRC), NSF Award number EEC-0813570 (YC, EB, ERO, LK, VB, CG, ZS, JD and LJ), by NSF Award number CBET-1511646 (AW, ZS and LJ), National Institutes of Health R01 GM37048 (WR and RG) and the Karen and Denny Vaughn Faculty Fellowship (TM and LJ). The funders had no role in study design, data collection and analysis, decision to publish, or preparation of the manuscript. We thank the Iowa State University (ISU) W.M. Keck Metabolomics Research Laboratory for help with membrane polarization and GC-MS analysis, ISU DNA Facility for help with whole-genome sequencing, and ISU Flow Cytometry Facility for the help with SYTOX Green cells analysis.

6. References

Abranches, J., Martinez, A. R., Kajfasz, J. K., Chavez, V., Garsin, D. A., Lemos, J. A., 2009. The Molecular Alarmone (p)ppGpp Mediates Stress Responses, Vancomycin Tolerance, and Virulence in *Enterococcus faecalis*. Journal of Bacteriology. 191**,** 2248-2256.

Atsumi, S., Wu, T. Y., Machado, I. M. P., Huang, W. C., Chen, P. Y., Pellegrini, M., Liao, J. C., 2010. Evolution, genomic analysis, and reconstruction of isobutanol tolerance in *Escherichia coli*. Molecular Systems Biology. 6.

Chen, Y. X., Reinhardt, M., Neris, N., Kerns, L., Mansell, T. J., Jarboe, L. R., 2018. Lessons in Membrane Engineering for Octanoic Acid Production from Environmental *Escherichia coli* Isolates. Applied and Environmental Microbiology. 84.

Chueca, B., Renzoni, A., Berdejo, D., Pagan, R., Kelley, W. L., Garcia-Gonzalo, D., 2018. Whole-Genome Sequencing and Genetic Analysis Reveal Novel Stress Responses to Individual Constituents of Essential Oils in *Escherichia coli*. Applied and Environmental Microbiology. 84.

Desbois, A. P., Smith, V. J., 2010. Antibacterial free fatty acids: activities, mechanisms of action and biotechnological potential. Applied Microbiology and Biotechnology. 85**,** 1629-1642.

Dunlop, M. J., 2011. Engineering microbes for tolerance to next-generation biofuels. Biotechnology for Biofuels. 4.

Fletcher, E., Pilizota, T., Davies, P. R., McVey, A., French, C. E., 2016. Characterization of the effects of n-butanol on the cell envelope of *E-coli*. Applied Microbiology and Biotechnology. 100**,** 9653-9659.

Foo, J. L., Jensen, H. M., Dahl, R. H., George, K., Keasling, J. D., Lee, T. S., Leong, S., Mukhopadhyay, A., 2014. Improving Microbial Biogasoline Production in *Escherichia coli* Using Tolerance Engineering. Mbio. 5.

Guan, N. Z., Li, J. H., Shin, H. D., Du, G. C., Chen, J., Liu, L., 2016. Metabolic engineering of acid resistance elements to improve acid resistance and propionic acid production of *Propionibacterium jensenii*. Biotechnology and Bioengineering. 113**,** 1294-1304.

Horinouchi, T., Sakai, A., Kotani, H., Tanabe, K., Furusawa, C., 2017. Improvement of isopropanol tolerance of *Escherichia coli* using adaptive laboratory evolution and omics technologies. Journal of Biotechnology. 255**,** 47-56.

Horinouchi, T., Suzuki, S., Hirasawa, T., Ono, N., Yomo, T., Shimizu, H., Furusawa, C., 2015. Phenotypic convergence in bacterial adaptive evolution to ethanol stress. BMC Evolutionary Biology. 15.

Jarboe, L. R., 2018. Improving the success and impact of the metabolic engineering design, build, test, learn cycle by addressing proteins of unknown function. Current Opinion in Biotechnology. 53**,** 93-98.

Jarboe, L. R., Klauda, J. B., Chen, Y., Davis, K. M., Santoscoy, M. C., 2018. Engineering the Microbial Cell Membrane to Improve Bioproduction. In: Cheng, H. N., Gross, R. A., Smith, P. B., Eds.), Green Polymer Chemistry: New Products, Processes and Applications. American Chemical Society, Washington, DC.

Jarboe, L. R., Liu, P., Royce, L. A., 2011. Engineering inhibitor tolerance for the production of biorenewable fuels and chemicals. Current Opinion in Chemical Engineering. 1**,** 38-42.

Jin, T., Chen, Y., Jarboe, L. R., 2016. Evolutionary Methods for Improving the Production of Biorenewable Fuels and Chemicals. In: Eckert, C., Trinh, C., Eds.), Biotechnology for Biofuels Production and Optimization. Elsevier.

Jin, T., Rover, M. R., Petersen, E. M., Chi, Z., Smith, R. G., Brown, R. C., Wen, Z., Jarboe, L. R., 2017. Damage to the microbial cell membrane during pyrolytic sugar utilization and strategies for increasing resistance. Journal of Industrial Microbiology & Biotechnology. 44**,** 1279-1292.

Jing, F. Y., Cantu, D. C., Tvaruzkova, J., Chipman, J. P., Nikolau, B. J., Yandeau-Nelson, M. D., Reilly, P. J., 2011. Phylogenetic and experimental characterization of an acyl-ACP thioesterase family reveals significant diversity in enzymatic specificity and activity. Bmc Biochemistry. 12.

Korstanje, T. J., van der Vlugt, J. I., Elsevier, C. J., de Bruin, B., 2015. Hydrogenation of carboxylic acids with a homogeneous cobalt catalyst. Science. 350**,** 298-+.

Laughrea, M., Latulippe, J., Filion, A. M., 1984. Effect of ethanol, phenol, formamide, dimethylsulfoxide, paromomycin, and deuterium-oxide on the fidelty of translation in a brain cell-free system. Biochemistry. 23**,** 753-758.

Lennen, R., Nielsen, A. T., Herrgard, M., Sommer, M. O. A., Feist, A., Tharwat Tolba Mohamed, E., Bacterial cells with improved tolerance to diacids. In: Bureau, W. I. P. O. I., (Ed.). Danmarks Tekniske Universitet, Denmark, 2018.

Lennen, R. M., Jensen, K., Mohammed, E. T., Malla, S., Borner, R. A., Chekina, K., Ozdemir, E., Bonde, I., Koza, A., Maury, J., Pedersen, L. E., Schoning, L. Y., Sonnenschein, N., Palsson, B. O., Sommer, M. O. A., Feist, A. M., Nielsen, A. T., Herrgard, M., Sommer,

M. O. A., Markus, J. H., Adaptive laboratory evolution reveals general and specific chemical tolerance mechanisms and enhances biochemical production. bioRxiv, 2019.

Lennen, R. M., Kruziki, M. A., Kumar, K., Zinkel, R. A., Burnum, K. E., Lipton, M. S., Hoover, S. W., Ranatunga, D. R., Wittkopp, T. M., Marner, W. D., Pfleger, B. F., 2011. Membrane Stresses Induced by Overproduction of Free Fatty Acids in *Escherichia coli*. Applied and Environmental Microbiology. 77**,** 8114-8128.

Lennen, R. M., Pfleger, B. F., 2013. Modulating Membrane Composition Alters Free Fatty Acid Tolerance in *Escherichia coli*. Plos One. 8.

Li, M., Zhang, X. J., Agrawal, A., San, K. Y., 2012. Effect of acetate formation pathway and long chain fatty acid CoA-ligase on the free fatty acid production in *E. coli* expressing acy-ACP thioesterase from *Ricinus communis*. Metabolic Engineering. 14**,** 380-387.

Lian, J., McKenna, R., Rover, M. R., Nielsen, D. R., Wen, Z., Jarboe, L. R., 2016. Production of biorenewable styrene: utilization of biomass□derived sugars and insights into toxicity. Journal of Industrial Microbiology & Biotechnology. 43**,** 595-604.

Liang, X., Liao, C. Y., Thompson, M. L., Soupir, M. L., Jarboe, L. R., Dixon, P. M., 2016. *E. coli* Surface Properties Differ between Stream Water and Sediment Environments. Frontiers in Microbiology. 7.

Liao, C., Liang, X., Soupir, M. L., Jarboe, L. R., 2015. Cellular, particle and environmental parameters influencing attachment in surface waters: a review. Journal of Applied Microbiology. 119**,** 315-330.

Liu, P., Chernyshov, A., Najdi, T., Fu, Y., Dickerson, J., Sandmeyer, S., Jarboe, L., 2013. Membrane stress caused by octanoic acid in *Saccharomyces cerevisiae*. Applied Microbiology and Biotechnology. 97**,** 3239-3251.

Lopez-Ruiz, J. A., Davis, R. J., 2014. Decarbonylation of heptanoic acid over carbon-supported platinum nanoparticles. Green Chemistry. 16**,** 683-694.

Luo, L. H., Seo, P. S., Seo, J. W., Heo, S. Y., Kim, D. H., Kim, C. H., 2009. Improved ethanol tolerance in *Escherichia coli* by changing the cellular fatty acids composition through genetic manipulation. Biotechnology Letters. 31**,** 1867-1871.

Mitchell, J. J., Lucaslenard, J. M., 1980. The effect of alcohols on guanosine 5'-diphosphate-3'0diphosphate metabolism in stringent and relaxied *Escherichia coli*. Journal of Biological Chemistry. 255**,** 6307-6313.

Nagahama, H., Sakamoto, Y., Matsumoto, K., Hara, H., 2006. RcsA-dependent and -independent growth defects caused by the activated Rcs phosphorelay system in the *Escherichia coli pgsA* null mutant. Journal of General and Applied Microbiology. 52**,** 91-98.

Nguyen, M. T., Hanzelmann, D., Hartner, T., Peschel, A., Gotz, F., 2016. Skin-Specific Unsaturated Fatty Acids Boost the *Staphylococcus aureus* Innate Immune Response. Infection and Immunity. 84**,** 205-215.

Ogasawara, H., Shinohara, S., Yamamoto, K., Ishihama, A., 2012. Novel regulation targets of the metal-response BasS-BasR two-component system of *Escherichia coli*. Microbiology-Sgm. 158**,** 1482-1492.

Parker, C. T., Kloser, A. W., Schnaitman, C. A., Stein, M. A., Gottesman, S., Gibson, B. W., 1992. Role of the *rfaG* and *rfaP* genes in determining the lipopolysaccharide core structure and cell-surface properties of *Escherichia coli* K-12. Journal of Bacteriology. 174**,** 2525-2538.

Qi, Y. L., Liu, H., Chen, X. L., Liu, L. M., 2019. Engineering microbial membranes to increase stress tolerance of industrial strains. Metabolic Engineering. 53**,** 24-34.

Ren, G., Wang, Z., Li, Y., Hu, X. Q., Wang, X. Y., 2016. Effects of Lipopolysaccharide Core Sugar Deficiency on Colanic Acid Biosynthesis in *Escherichia coli*. Journal of Bacteriology. 198**,** 1576-1584.

Reyes, L. H., Almario, M. P., Winkler, J., Orozco, M. M., Kao, K. C., 2012. Visualizing evolution in real time to determine the molecular mechanisms of n-butanol tolerance in *Escherichia coli*. Metabolic Engineering. 14**,** 579-590.

Rosenberg, M., Gutnick, D., Rosenberg, E., 1980. Adhyerence of bacteria to hydrocarbons - a simple method for measuring cell-surface hydrophobicity. Fems Microbiology Letters. 9**,** 29-33.

Ross, W., Sanchez-Vazquez, P., Chen, A. Y., Lee, J. H., Burgos, H. L., Gourse, R. L., 2016. ppGpp Binding to a Site at the RNAP-DksA Interface Accounts for Its Dramatic Effects on Transcription Initiation during the Stringent Response. Mol. Cell. 62**,** 811-823.

Ross, W., Vrentas, C. E., Sanchez-Vazquez, P., Gaal, T., Gourse, R. L., 2013. The Magic Spot: A ppGpp Binding Site on *E. coli* RNA Polymerase Responsible for Regulation of Transcription Initiation. Mol. Cell. 50**,** 420-429.

Roth, B. L., Poot, M., Yue, S. T., Millard, P. J., 1997. Bacterial viability and antibiotic susceptibility testing with SYTOX Green nucleic acid stain. Applied and Environmental Microbiology. 63**,** 2421-2431.

Royce, L., Boggess, E., Jin, T., Dickerson, J., Jarboe, L., 2013a. Identification of mutations in evolved bacterial genomes. Methods in molecular biology (Clifton, N.J.). 985**,** 249-67.

Royce, L. A., Liu, P., Stebbins, M. J., Hanson, B. C., Jarboe, L. R., 2013b. The damaging effects of short chain fatty acids on *Escherichia coli* membranes. Applied Microbiology and Biotechnology. 97**,** 8317-8327.

Royce, L. A., Yoon, J. M., Chen, Y., Rickenbach, E., Shanks, J. V., Jarboe, L. R., 2015. Evolution for exogenous octanoic acid tolerance improves carboxylic acid production and membrane integrity. Metabolic Engineering. 29**,** 180-188.

Sanchez-Vazquez, P., Dewey, C. N., Kitten, N., Ross, W., Gourse, R. L., 2019. Genome-wide effects on *Escherichia coli* transcription from ppGpp binding to its two sites on RNA polymerase. Proceedings of the National Academy of Sciences of the United States of America. 116**,** 8310-8319.

Sandoval, N. R., Mills, T. Y., Zhang, M., Gill, R. T., 2011. Elucidating acetate tolerance in *E. coli* using a genome-wide approach. Metabolic Engineering. 13**,** 214-224.

Sandoval, N. R., Papoutsakis, E. T., 2016. Engineering membrane and cell-wall programs for tolerance to toxic chemicals: Beyond solo genes. Current Opinion in Microbiology. 33**,** 56-66.

Sherkhanov, S., Korman, T. P., Bowie, J. U., 2014. Improving the tolerance of *Escherichia coli* to medium-chain fatty acid production. Metabolic Engineering. 25**,** 1-7.

So, A. G., Davie, E. W., 1964. Effects of organic solvents on protein biosynthesis + their influence on amino acid code. Biochemistry. 3**,** 1165-+.

Tan, Z. G., Khakbaz, P., Chen, Y. X., Lombardo, J., Yoon, J. M., Shanks, J. V., Klauda, J. B., Jarboe, L. R., 2017. Engineering Escherichia coli membrane phospholipid head distribution improves tolerance and production of biorenewables. Metabolic Engineering. 44**,** 1-12.

Tan, Z. G., Yoon, J. M., Nielsen, D. R., Shanks, J. V., Jarboe, L. R., 2016. Membrane engineering via trans unsaturated fatty acids production improves *Escherichia coli* robustness and production of biorenewables. Metabolic Engineering. 35**,** 105-113.

Tee, T. W., Chowdhury, A., Maranas, C. D., Shanks, J. V., 2014. Systems Metabolic Engineering Design: Fatty Acid Production as an Emerging Case Study. Biotechnology and Bioengineering. 111**,** 849-857.

Thomason, L. C., Costantino, N., Court, D. L., 2014. *E. coli* Genome Manipulation by P1 Transduction. Current Protocols. 79.

Van Dien, S., 2013. From the first drop to the first truckload: commercialization of microbial processes for renewable chemicals. Current Opinion in Biotechnology. 24**,** 1061-1068.

Venkataramanan, K. P., Kurniawan, Y., Boatman, J. J., Haynes, C. H., Taconi, K. A., Martin, L., Bothun, G. D., Scholz, C., 2014. Homeoviscous response of *Clostridium pasteurianum* to butanol toxicity during glycerol fermentation. Journal of Biotechnology. 179**,** 8-14.

Wang, Z., Wang, J. L., Ren, G., Li, Y., Wang, X. Y., 2015. Influence of Core Oligosaccharide of Lipopolysaccharide to Outer Membrane Behavior of *Escherichia coli*. Marine Drugs. 13**,** 3325-3339.

Yang, X. M., Ishiguro, E. E., 2003. Temperature-sensitive growth and decreased thermotolerance associated with *relA* mutations in *Escherichia coli*. Journal of Bacteriology. 185**,** 5765-5771.

Yethon, J. A., Vinogradov, E., Perry, M. B., Whitfield, C., 2000. Mutation of the lipopolysaccharide core glycosyltransferase encoded by *waaG* destabilizes the outer membrane of *Escherichia coli* by interfering with core phosphorylation. Journal of Bacteriology. 182**,** 5620-5623.

Zhang, H. F., Chong, H. Q., Ching, C. B., Song, H., Jiang, R. R., 2012. Engineering global transcription factor cyclic AMP receptor protein of *Escherichia coli* for improved 1-butanol tolerance. Applied Microbiology and Biotechnology. 94**,** 1107-1117.

Zhang, X. S., Garcia-Contreras, R., Wood, T. K., 2008. *Escherichia coli* transcription factor YncC (McbR) regulates colanic acid and biofilm formation by repressing expression of periplasmic protein YbiM (McbA). Isme Journal. 2**,** 615-631.

Zuo, Y. H., Wang, Y. M., Steitz, T. A., 2013. The Mechanism of *E. coli* RNA Polymerase Regulation by ppGpp Is Suggested by the Structure of their Complex. Mol. Cell. 50**,** 430-436.

Table 1: Identification and timing of mutations acquired during evolution for C8 tolerance in minimal media at pH 7.0. Evolution of ML115 to strains LAR1 and LAR2 was previously described (Royce et al., 2015) over the course of 17 sequential transfers, with LAR1 and LAR2 both isolated as single colonies from the same final liquid culture. Timing of mutations was determined by PCR and restriction analysis of samples archived during the sequential transfers.

Table 2: Restoration of *waaG* and mutation of *rpoC* and *basR* in parent strain ML115 reproduces the phenotype of evolved strain LAR1 during challenge with exogenous C8. Cells were grown in minimal media at 37°C with 1.5 wt% dextrose with an initial pH of 7.0. Growth measurements were taken hourly. Shading from black to red indicates the degree of reconstitution of the evolved strain genotype. Values are the average of three replicates with the associated standard deviation. [a] $p \leq 0.0038$ relative to LAR1, [b] $p < 0.0038$ relative to ML115

Figure 1. Views of a section of the crystal structure of *E. coli* RNA polymerase showing location of RpoC H419 adjacent to binding site 1 for ppGpp (adapted in PyMOL from PDB 4JKR (Zuo et al., 2013)). (A) RpoC H419 (yellow spheres) is adjacent to ppGpp binding site 1. ppGpp: red spheres. Portions of the RNAP subunits RpoC (β', light pink); RpoB (β, light blue), RpoZ (ω, teal), and RpoA (α, grey) are shown in cartoon form. Residues shown biochemically and genetically to be required for ppGpp function at site 1 (Ross et al., 2013) are shown as blue spheres (RpoC R417, K615, R362, D622, Y626), and teal spheres (RpoZ A2, R3, V4). (B) RpoC H419 and ppGpp binding site 1 are located 30Å from the RNAP active site. View is rotated from that in (A) to show the active site Mg^{2+} (magenta sphere). Other colors are as for (A).

Figure 2. Restoration of *waaG* (*waaG*^{R}) and mutation of *rpoC* (*rpoC*^{H419P}) reproduce the increased fatty acid titer of evolved strain LAR1. All strains contain plasmid pJMY-EEI82564 encoding the *A. tetradius* thioesterase (TE10). Strains were grown in LB with 1.5 wt% dextrose at 30°C, 250 rpm with 100 mg/L ampicillin and 1.0 mM IPTG. (A) Fatty acid titer after 72 hours. (B) Strain growth during fatty acid production. Values are the average of three biological replicates, with error bars indicating one standard deviation. A titer of 1 g/L corresponds to approximately 7 mM.

Figure 3. Each of the mutations contributes to changes in the cell membrane. Cells were assessed after challenge with exogenous C8 at pH 7.0 and 37°C. Data for the *waaG*^{R} strain is shown twice to support comparison of strains. (A) Membrane integrity was assessed via permeability to the SYTOX nucleic acid dye. (B) Membrane rigidity was characterized via DPH polarization. (C) Average length of the membrane lipid tails. (D) Cell surface hydrophobicity. Membrane permeability, rigidity and hydrophobicity were assessed after challenge with 10 mM C8. Average lipid length was assessed after challenge with 30 mM C8.

Figure 4: Restoration of WaaG affects (A) production of extracellular polysaccharides, (B) colony morphology, and (C) production of flagella.
*indicates a significant difference ($p \leq 0.01$) from LAR1

Figure 5: RpoC^{H419P} impacts tolerance to a variety of inhibitors, possibly by affecting interaction of RpoC and ppGpp. Unless otherwise indicated, cells were grown at 37°C in MOPS minimal media containing 2.0 wt% dextrose and the indicated inhibitor and with an initial pH of 7.0.
(A) Replacement of *rpoC* with *rpoC*^{H419P} in ML115+*waaG*^{R} impacts tolerance to a variety of inhibitors. This analysis compares strains YC001 and YC005.
(B) The RpoC site 1 mutation also impacts tolerance relative to the corresponding isogenic control strain. Data for RpoC^{H419} is reproduced from Figure 5A, comparing strains YC001 and YC005. Data for the site 1 mutant compares previously characterized strain RLG14536 lacking site 1 (RpoC R362A, R417A, K615A, RpoZ Δ2-5) to its corresponding control RLG14535. The indicated p-values compare the magnitude of the increase in specific growth rate due to *rpoC*^{H419P} to the increase in specific growth rate due to the site 1 null mutation (1-2+).
(C) RpoC^{H419P} does not delay recovery from nutrient downshift. ML115+*waaG*^{R} with either the wild-type version of *rpoC* (YC001) or *rpoC*^{H419P} (YC005) was grown at 30°C in LB and then washed and resuspended in either LB or MOPS minimal growth medium.

Figure 6: Proposed summary of how mutations in WaaG, RpoC and the BasS-BasR system impact tolerance of octanoic acid and membrane integrity, hydrophobicity, rigidity and composition.

Supplemental Materials and Methods

Strains, plasmids and bacterial cultivation

All strains and plasmids used in this study are listed in Tables S1 and S2. *E. coli* DH5α strain was used as a cloning strain. Overnight seed cultures were grown in 250 mL flasks with 25 mL of MOPS minimal media (Neidhardt et al., 1974) with 2.0 wt% dextrose at pH 7.00±0.05, 37 ˚C, and 250 rpm. The overnight cultures were diluted to an optical density at 550 nm (OD_{550}) of 0.05 for the octanoic acid tolerance test, or to an OD_{550} of 0.1 for testing membrane leakage, membrane fluidity, cell hydrophobicity, and cell membrane composition. Chloramphenicol (35 mg/L), ampicillin (100 mg/L), kanamycin (50 mg/L), and spectinomycin (50 mg/L) were added as needed.

Whole-genome sequencing and verification of mutations

Genomic DNA was purified using the Qiagen (Hilden, Germany) Blood and Tissue kit. The Illumina Genome Analyzer II platform for high throughput sequencing was used for whole genome sequencing at the Iowa State University DNA facility with 77-base pair (bp) paired-end reads, as previously described (Royce et al., 2013a). The software and algorithms used for genome assembly and identifying mutations were previously described (Royce et al., 2013a). Breseq (version 0.31.0), a pipeline for finding mutations in microbial genomes, was used to analyze the short read data (Deatherage and Barrick, 2014). Breseq aligns reads to a reference genome, in our case wild-type *E. coli* K-12 MG1655 U00096.3 (Blattner et al., 1997), using the Bowtie2 (version 2.3.3) alignment algorithm (Langmead and Salzberg, 2012) and R (version 3.4.1) (Team, 2018).

Genomes of the evolved and parent strains were aligned to the wild-type genome and variations in the evolved strain that were not present in the parental strain were verified by

Sanger sequencing. For all potential mutations, the entire associated gene, as well as 500 base pairs (bp) upstream and downstream, were sequenced. All primers were designed by primer3 (Untergasser et al., 2012) and synthesized by Integrated DNA Technologies (Coralville, Iowa, USA) (Table S3). PCR products were purified by QIAquick PCR purification kits (Qiagen) and sequenced at the Iowa State University DNA facility.

PCR-Restriction Fragment Length Polymorphism (PCR-RFLP)

Frozen stocks from the adaptive evolution (Royce et al., 2015) were used as template DNA for PCR. For the *rpoC*^{H419P} (A1256C) mutation, a 660 bp DNA fragment including position 1256 was amplified by PCR with the primers rpoCCF, rpoCCR using DreamTaq Green PCR master mix (Thermo Fisher Scientific, Waltham, MA). PCR products were purified by DNA Clean & Concentrator kit (Zymo Research, Irvine, CA, USA). Approximately 10 µl of purified PCR product was digested with restriction enzyme BsaJI (New England Biolabs, Ipswich, MA, USA) according to the manufacturer's instruction. The restriction fragments were separated on a 1 wt% TAE agarose gel with 1 Kb Plus DNA ladder (Invitrogen, Carlsbad, CA, USA). Similar analysis was performed for the *basS* and *basR* mutations, using primers basRCF and basRCR and restriction enzyme SfcI for *basR* and primers basSCF and basSCR and restriction enzyme FatI for *basS*. For the *waaG* mutation, waaGCF and waaGCR primers were used and PCR product was analyzed simply by size without restriction digestion.

Genomic manipulations

All genomic manipulations were carried out using either Lambda Red recombinase system (Datsenko and Wanner, 2000) or CRISP-cas9 system (Jiang et al., 2015). The rpoC(1256A)+kan, and rpoC(1256C)+kan cassettes were synthesized by GenScript (Piscataway, NJ, USA). The purified PCR products were transformed into the electro-competent *E. coli* cells

harboring pKD46 and grown in the presence of 2.0 mM L-arabinose to induce the Lambda red recombinase system. The resulting kanamycin resistant colonies were screened for successful gene replacement by the PCR amplification and DNA sequencing. The scarless CRISPR-Cas9 approach was also applied to perform gene editing (Jiang et al., 2015).

Assessment of inhibitor tolerance and nutrient downshift

Overnight seed cultures were inoculated into 250 mL baffled flasks with 25 mL MOPS with 2.0 wt% dextrose and the relevant inhibitor. Unless stated otherwise, growth was performed at 37°C and 200 rpm and the media pH was adjusted to 7.00±0.05 with 2.0M KOH or 1.0M HCl. Octanoic acid (C8) was provided via a 4.0 M stock solution in 100 % ethanol. Other inhibitors were added to the following concentrations: 10 mM hexanoic acid (C6); 600 mM NaCl; 65.6 mM levulinic acid; 200 mM citrate; 54.3 mM sodium formate; 11.9 mM hydroxybenzoate; 3.6 mM trans-ferulic acid; 0.6% v/v n-butanol; 0.6% v/v iso-butanol; 2% v/v ethanol; 200 mM succinate; 6.6 mM vanillin; 10.4 mM furfural; 9.3% w/v glucose. OD_{550} was measured approximately every hour and mid-log data was fitted to an exponential curve, with a line of fit $R^2 \geq 0.9$.

Nutritional downshift was performed as previously described (Ross et al., 2013). Briefly, cells were grown to OD 0.6 – 0.8 in LB with 1.0 wt% dextrose at 30°C, washed in MOPS minimal medium with 2.0 wt% dextrose, and resuspended in either fresh LB with 1.0 wt% dextrose or MOPS minimal medium with 2.0 wt% dextrose and grown at 30°C. Downshift experiments were performed in 96-well plates with a total well volume of 200 µL and initial OD of 0.1. Incubations were carried out in a Synergy HT plate reader with shaking at 405 cycles per minute for 24 hours.

Fatty acid production

Strains transformed with the pJMY-EEI82564 plasmid were grown on LB plates with ampicillin and incubated at 30°C overnight. Individual colonies were cultured in 250 mL flasks in 10 mL LB with ampicillin at 30°C on a rotary shaker at 250 rpm overnight. Seed cultures were inoculated at an approximate OD_{550} of 0.1 into 250 mL baffled flasks containing 50 mL of LB with 1.5 wt% dextrose, ampicillin, and 1.0 mM isopropyl-β-D-thiogalactopyranoside (IPTG). The flasks were incubated in a rotary shaker at 250 rpm and 30°C.

Fatty acids were extracted and further derivatized from samples containing both media and cells. The fatty acid methyl esters (FAMEs) were measured with an Agilent 6890 Gas Chromatograph coupled to an Agilent 5973 Mass Spectrometer (GC-MS) at the ISU W.M. Keck Metabolomics Research Laboratory, as previously described (Torella et al., 2013). Briefly, 1 mL culture was transferred into a 2 mL microcentrifuge tube, and 125 µL 10% NaCl (w/v), 125 µL acetic acid, 20 µL internal standard (1 µg/µL C7, C11, C15 in ethanol), 500 µL ethyl acetate were added sequentially. The mixture was vortexed for 30 s and centrifuged at 16,000×g for 10 min. Then, 250 µL of the top layer, containing the free fatty acids, was transferred into a glass tube. To derivatize the fatty acids, 2.25 mL 30:1 EtOH: 37% HCl (v/v) was added, and the mixture incubated at 55ºC for 1 hour, then cooled to room temperature. Then 1.25 mL each ddH_2O and hexane were added, followed by vortexing and centrifugation at 2,000×g for 2 min. The top layer (hexane) was then analyzed by GC-MS using the following programs: the initial temperature was set at 50°C, hold for 1 min, with the following temperature ramp: 20 °C/min to 140°C, 4°C/min to 220°C, and 5°C/min to 280°C with 1 ml/min helium as carrier gas. The relative retention factor of C7/C11/C15 was used to adjust the relative amounts of the individual

fatty acids analyzed. The Enhanced Data Analysis (Agilent Technologies) and NIST 17 Mass Spectral Library software were used for peak identification.

Extracellular polymeric substance (EPS) extraction and quantification

The total extracellular protein and polysaccharide were determined as previously described (Liang et al., 2016). Briefly, cells were grown on LB agar plates overnight at 37°C to obtain 2×10^{11} - 4×10^{11} cells, suspended in 30 mL 0.85 wt% NaCl solution and quantified via CountBright absolute counting beads (ThermoFisher Scientific), at the Iowa State University Flow Cytometry Facility. The cell suspension was centrifuged at 16,300×g, at 4°C for 30 min, the supernatant was passed through a 0.45 µm filter and 90 mL of ice-cold 100% ethanol was added. The mixture was incubated at -20°C for 24 h. Then, the EPS pellet was harvested by centrifuging at 16,300×g for 30 min at 4°C, drying at room temperature and resuspension in 20 mL DI water. The Lowry method (Lowry et al., 1951) was used to quantify protein content, using bovine serum albumin (Sigma-Aldrich, St. Louis, MO, USA) as the standard. The phenol-sulfuric acid method was used to analyze EPS sugar (Dubois et al., 1956), using xanthan gum as the standard.

Colony morphology

Cells were streaked onto LB plates from frozen stock with chloramphenicol, incubated at 37°C overnight, and then incubated at room temperature for an additional 24 hours. Colonies were then photographed to document differences in colony morphology.

TEM imaging

Cells were grown to mig-log phase ($OD_{550}\approx1$) in 25 mL of MOPS 2.0 wt% dextrose in 250 mL flasks with shaking at 37°C and 250 rpm and harvested by centrifugation at 4,500×g and room temperature for 10 min. Cells were washed twice with PBS pH 7.00±0.05 and resuspended

to OD_{550}~1 in PBS containing 10 mM octanoic acid at pH 7.0 and then incubated at 37°C for 1 hour. The control group was treated with PBS in the absence of C8. The resuspended cell solution was send to Roy J. Carver High Resolution Microscopy Facility at Iowa State University for transmission electron microscope (TEM) imaging.

Membrane characterization

For assessment of membrane permeability and DPH polarization, cells were grown, harvested and treated using the same produced described above for the TEM imaging. After incubation, cells were centrifuged at 4,500×g at 22°C for 10 min, washed twice with PBS, and resuspended in PBS at a final OD_{550}~1.

For characterization of membrane permeability, 100 µL of the cell suspension were diluted with 900 µL PBS and stained with 1 µL of 5mM SYTOX Green (Invitrogen, Carlsbad, CA) in dimethyl sulfoxide (Roth et al., 1997; Santoscoy and Jarboe, 2019). The stained cells were analyzed by flow cytometry with a BD Biosciences FACSCanto II, at the ISU Flow Cytometry facility. Approximately 18,000 events were tested per sample, and each sample had three parallel groups.

For measurement of DPH polarization, 500 µL of cell suspension was mixed with 500 µL of 0.4 µM 1,6-diphenyl-1, 3, 5-hexatirene (DPH, Life Technologies, Carlsbad, CA, USA) in PBS (Mykytczuk et al., 2007; Royce et al., 2013b). The mixture was vortexed and incubated in the dark at 37°C for 30 min. The treated cells were harvested by centrifugation at 5,000×g for 5 min and the cell pellets were resuspended in 500 µL PBS. From this mixture, 100 µL of this mixture was transferred into black-bottom Nunclon™ Delta surface 96-well plates with 4 replicates. A suspension of cells without DPH was used as control. Membrane fluorescence polarization values were determined based on vertical and horizontal fluorescence readings by the BioTek

Synergy 2 Multi-Mode microplate reader at ISU W.M. Keck Metabolomics Research Laboratory.

Measurement of cell surface hydrophobicity was performed as previously described (Rosenberg et al., 1980). The mid-log cells were harvested and treated with MOPS with 2.0 wt% dextrose with or without 10 mM octanoic acid, at pH 7.0 and 37°C with rotary shaking at 250 rpm for 1 hour. Cells were then washed twice in PBS and resuspended in PBS at a final OD_{550} ~ 0.6. Four mL of cell suspension were added to a glass tube, and the OD_{550} was measured as OD_1. Then, 1.0 mL of dodecane was added, and the mixture was vortexed using a multi-tube vortexer (Thermo Fisher Scientific Inc., Waltham, MA, USA) at 2500 rpm for 10 minutes. The mixture was left at room temperature for 15 min to allow phase separation. The OD_{550} of the aqueous phase (OD_2) was then measured. Partitioning of the bacteria suspension was calculated as:

Percent partitioning = $[(OD_1-OD_2)/OD_1]*100$

For measurement of membrane lipid composition, cells were grown to mid-log phase, harvested and resuspended in MOPS 2.0 wt% dextrose with or without 30 mM octanoic acid at pH 7.0, and incubated for 3 hours at 37°C. Cells were washed twice with cold sterile water and resuspended in 6 mL methanol. 1.4 mL of cell suspension was transferred into glass tubes with three replicates (Bligh and Dyer, 1959). Twenty µL of 1 µg/µL C7, C11, C15 in methanol was added as internal standard. The mixtures were sonicated for three 30 s bursts, incubated at 70°C for 15 min, and cooled to room temperature. The mixture was then centrifuged at 4,000×g for 5 min. The supernatant was transferred into a new glass tube with 1.4 mL nanopure water, and the mixture was vortexed. After removal of the supernatant, the pellet was resuspended in 750 µL of chloroform by vortexing, followed by horizontal shaking at 150 rpm and 37°C for 5 min. The aqueous dilution of the supernatant was then added back to the chloroform-treated pellet. The

mixture was vortexed for 2 min, then centrifuged at 3,000×g for 5 min. The bottom layer (chloroform) contained free fatty acids and was transferred to a new glass tube. All solvent was removed by an N-Evap nitrogen tree evaporator. For fatty acid derivatization, 2.0 mL of 1.0 N HCl in methanol was added to the dried samples, heated at 80°C for 30 min, then cooled to room temperature. Then, 2.0 mL of 0.9 wt% NaCl and 1.0 mL hexane were added, followed by vortexing for 2 min and centrifugation at 2,000×g for 2 min. The upper layer containing the hexane with FAMEs was analyzed by GC-MS, as described above. The weight-average lipid length was calculated as previously described (Royce et al., 2013b).

Visualization of $RpoC^{H419P}$ mutation

Views of *E. coli* RNA polymerase showing the location of the $RpoC^{H419P}$ mutation (Figure 1) were adapted from the crystal structure of *E. coli* RNAP with ppGpp bound at site 1 (PDB 4JKR; (Zuo et al., 2013)), using PyMOL molecular visualization software.

Table S1. Strains used in this study

Strain	**Characteristics**				**Reference/ Source**
DH5α	Cloning host for constructing plasmids				New England Biolabs, Inc
ML115	MG1655 Δ*fadD*, Δ*poxB*, Δ*ackA-pta*				(Li et al., 2012)
RLG 14535	MG1655 *rpoZ*(WT)-*kanR*, *rpoC*(WT)-*tetAR* (1+2+)				(Ross et al., 2016)
RLG 14536	MG1655 *rpoZ*Δ2-5-*kanR*, *rpoC* R362A R417A K615A-*tetAR* (1-2+)				(Ross et al., 2016)
	Mutant gene				
	waaG^{R}	*rpoC*^{H419P}	*basR**	*basS**	
ML115					(Li et al., 2012)
LAR1	●	●	●		(Royce et al., 2015)
YC001: ML115+*waaG*^{R}	●				this study
YC002: ML115+*rpoC*^{H419P}		●			this study
YC003: ML115+*basR**			●		this study
YC004: ML115+*basS**				●	this study
YC005: ML115+*waaG*^{R}+*rpoC*^{H419P}	●	●			this study
YC006: ML115+*waaG*^{R}+*basR**	●		●		this study
YC007: ML115+*waaG*^{R}+*basS**	●			●	this study
YC008: ML115+*rpoC*^{H419P}+*basR**		●	●		this study
YC009: ML115+*basR**+*basS**			●	●	this study
YC010: ML115+*waaG*^{R}+*rpoC*^{H419P}+*basR**	●	●	●		this study
YC011: ML115+*waaG*^{R}+*basR**+*basS**	●		●	●	this study
YC012: LAR1+*waaG*^{R}+*rpoC*+*basR**	●		●		this study

Table S2. Plasmids used in this study

Plasmids	Characteristics or Descriptions	Reference
pJMY-EEI82564	pTrc-EEI82564 thioesterase (TE10) from *Anaerococcus tetradius*, Amp^R	(Royce et al., 2015)
pKD4	FRT-Kan-FRT cassette template, Amp^R, Kan^R	(Datsenko and Wanner, 2000)
pKD46	λ Red recombinase expression plasmid , Amp^R	(Datsenko and Wanner, 2000)
pCP20	FLP recombinase expression, AmpR, Cm^R	(Datsenko and Wanner, 2000)
pUC57-*rpoC*1256A	*rpoC*-1256A-FRT-Kan-FRT cassette template, Kan^R	this study
pUC57-*rpoC*1256C	*rpoC*-1256C-FRT-Kan-FRE cassette template, Kan^R	this study
pCas	*repA101*(Ts) *kan* P_{cas}-*cas9* P_{araB}-*Red* *lacI*^{q} P_{trc}-*sgRNA-pMB1*, Kan^R	(Jiang et al., 2015)
pTarget-*pMB1*	*pMB1 aadA* sgRNA-pMB1	(Jiang et al., 2015)
pTargetF-*waaG*	*pMB1 aadA* sgRNA-*waaG*-N20	this study
pTargetF-*basS*-1	*pMB1 aadA* sgRNA-*basS*-N20-1	this study
pTargetF-*basS*-2	*pMB1 aadA* sgRNA-*basS*-N20-2	this study
pTargetF-*basR*-1	*pMB1 aadA* sgRNA-*basR*-N20-1	this study
pTargetF-*basR*-2	*pMB1 aadA* sgRNA-*basR*-N20-2	this study

Table S3. Primers used to verify mutations and establish the chronological order of mutations.

Primers	Sequence
rpoCCF	CCGGTCGTTCTGTAATCACC
rpoCCR	TCAGGCTGGTTTTCGCTACT
basRCF	CGCAAACGCAACACTATTCA
basRCR	GCCTGCTTTGAGCATTAACC
basSCF	GCGAAACCTGGTAGAAAACG
basSCR	AACATCCGCGAATTGATGA
waaGCF	GGAAAAGCTGTTGCCAGAAG
waaGCR	AGCATCTTTACCACGCCAAA

Table S4. Transcriptional analysis of components of the fatty acid biosynthesis initiation I, II and III and the fatty acid elongation – saturated, pathways, as classified and named by EcoCyc Pathway Tools version 23.0 (Keseler et al., 2017). Values are reproduced from (Sanchez-Vazquez et al., 2019) and indicate a fold change following induction of plasmid-borne *relA* in strains with (1+2+) or without (1-2-) the two binding sites for ppGpp on RNA polymerase.

Statistical categorization is as presented in (Sanchez-Vazquez et al., 2019), briefly summarized here: A (red) indicates statistically significant above 2-fold decrease. C (pink) indicates statistically significant under 2-fold decrease, D (light green) indicates statistically significant under 2-fold increase, and E (gray) indicates no significant change relative to the test strain. All values were deemed "trusted values" in the original analysis due to a lack of significant changes in the control strains and reads of sufficient length.

Gene	enzyme name	Synonym	1+2+ 5 min	1+2+ 5 min Category	1+2+ 10 min	1+2+ 10 min Category	1-2- 5 min	1-2- 5 min Category	1-2- 10 min	1-2- 10 min Category	1-2-/1+2+ 0 min	1-2-/1+2+ 0 min Category
accA	acetyl-CoA carboxyltransferase	b0185	-0.54	C	-1.25	A	-0.13	E	-0.28	C	-0.67	C
accD	acetyl-CoA carboxyltransferase	b2316	-0.60	C	-0.92	C	-0.04	E	-0.20	E	0.09	E
fabD	[acyl-carrier-protein] S-malonyltransferase	b1092	-0.59	C	-0.91	C	-0.15	E	-0.27	C	-0.10	E
fabH	beta-ketoacyl-ACP synthase	b1091	-1.00	C	-1.69	A	-0.26	C	-0.53	C	-0.33	C
fabF	acetoacetyl-[acp] synthase	b1095	-0.69	C	-1.39	A	-0.02	E	-0.18	C	0.11	D
fabB	acetoacetyl-[acp] synthase	b2323	-0.49	C	-0.13	E	0.22	E	0.08	E	0.06	E
fabG	3-oxoacyl-[acp] reductase	b1093	-0.46	C	-0.84	C	-0.07	E	-0.34	C	-0.20	C
fabZ	(3R)-3-hydroxyacyl-[acp] dehydratase	b0180	-0.80	C	-1.24	A	-0.12	E	-0.39	C	-0.32	C
fabA	3-hydroxylacyl-[acp] dehydratase	b0954	-0.61	C	-0.88	C	-0.01	E	0.01	E	0.25	D
fabI	2,3,4-saturated fatty acyl-[acp]:NAD+ oxidoreductase	b1288	-0.65	C	-1.03	A	-0.07	E	-0.26	C	-0.09	E

Supplemental Figure 1: PCR-Restriction Fragment Length Polymorphism uses to determine the order of mutations in evolved strains. Representative RFLP genotypes of the *waaG*, *rpoC*, *basS*, and *basR* genes fragment analysis using 1% agarose gel electrophoresis. Lanes 1 and 18 contain the 1 Kb Plus DNA Ladder (Invitrogen); lanes 2 and 17 contain PCR product from parent strain ML115 and evolved strain LAR1, respectively; lanes 3-16 contain PCR product from frozen stocks of successive transfers refers during directed evolution, with the transfer number indicated by the corresponding number.

(A) *waaG*, with removal of the insertion sequence and restoration of the functional gene sequence between transfers 2 and 3. The PCR product size with the insertion should be 1996 bp; the PCR products size of the *waaG* without the insertion should be 1219 bp.

(B) *rpoC*, with only the $rpoC^{H419P}$ sequence being detected by the 13th transfer. PCR product was subjected to digestion with BsaJI. Digestion of PCR product from the wild-type *rpoC* should be 427 bp and 233 bp, while digestion of PCR production of $rpoC^{H419P}$ should produce bands of length 208 bp, 219 bp, and 233 bp.

(C) *basS* mutation; PCR product was subjected to digestion with FatI. The wild-type sequence should produce bands sizes of 84 bp and 434 bp, while the mutant sequence should produce a single band of length 491 bp. Note that the *basS* mutation is present in strain LAR2 (not shown), and not LAR1, though an antecedent of LAR2 should be present in the 15th transfer.

(D) *basR* mutation; PCR product was subjected to digestion with SfcI. The band size for the wild-type *basR* should be 619 bp; the band sizes for the mutant *basR* should be 202 bp and 417 bp.

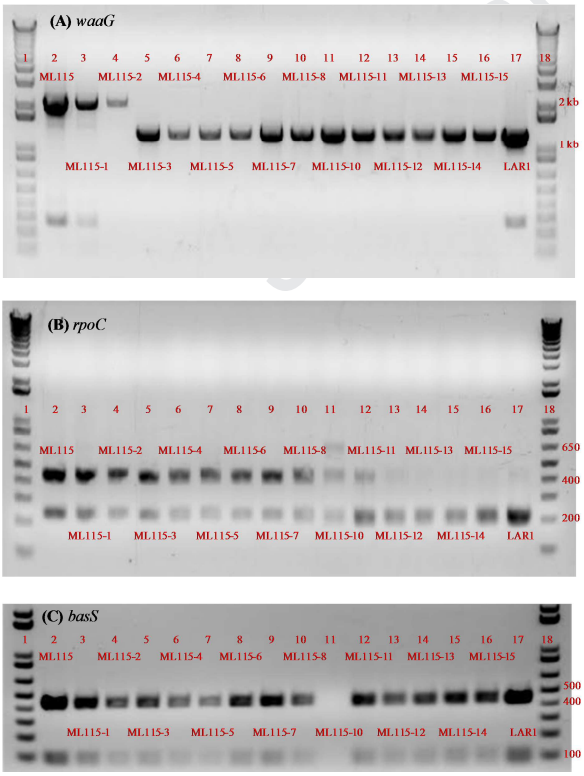

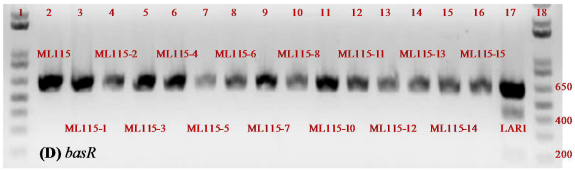

References

Blattner, F. R., Plunkett, G., Bloch, C. A., Perna, N. T., Burland, V., Riley, M., ColladoVides, J., Glasner, J. D., Rode, C. K., Mayhew, G. F., Gregor, J., Davis, N. W., Kirkpatrick, H. A., Goeden, M. A., Rose, D. J., Mau, B., Shao, Y., 1997. The complete genome sequence of *Escherichia coli* K-12. Science. 277**,** 1453-+.

Bligh, E. G., Dyer, W. J., 1959. A rapid method of total lipid extraction and purification. Canadian Journal of Biochemistry and Physiology. 37**,** 911-917.

Datsenko, K. A., Wanner, B. L., 2000. One-step inactivation of chromosomal genes in *Escherichia coli* K-12 using PCR products. Proceedings of the National Academy of Sciences of the United States of America. 97**,** 6640-6645.

Deatherage, D. E., Barrick, J. E., 2014. Identification of Mutations in Laboratory-Evolved Microbes from Next-Generation Sequencing Data Using breseq. In: Sun, L., Shou, W., Eds.), Engineering and Analyzing Multicellular Systems: Methods and Protocols. vol. 1151, pp. 165-188.

Dubois, M., Gilles, K. A., Hamilton, J. K., Rebers, P. A., Smith, F., 1956. Colorimetric method for determination of sugars and related substances. Analytical Chemistry. 28**,** 350-356.

Jiang, Y., Chen, B., Duan, C. L., Sun, B. B., Yang, J. J., Yang, S., 2015. Multigene Editing in the *Escherichia coli* Genome via the CRISPR-Cas9 System. Applied and Environmental Microbiology. 81**,** 2506-2514.

Keseler, I. M., Mackie, A., Santos-Zavaleta, A., Billington, R., Bonavides-Martinez, C., Caspi, R., Fulcher, C., Gama-Castro, S., Kothari, A., Krummenacker, M., Latendresse, M., Muniz-Rascado, L., Ong, Q., Paley, S., Peralta-Gil, M., Subhraveti, P., Velazquez-Ramirez, D. A., Weaver, D., Collado-Vides, J., Paulsen, I., Karp, P. D., 2017. The

EcoCyc database: reflecting new knowledge about *Escherichia coli* K-12. Nucleic Acids Research. 45**,** D543-D550.

Langmead, B., Salzberg, S. L., 2012. Fast gapped-read alignment with Bowtie 2. Nature Methods. 9**,** 357-U54.

Li, M., Zhang, X. J., Agrawal, A., San, K. Y., 2012. Effect of acetate formation pathway and long chain fatty acid CoA-ligase on the free fatty acid production in *E. coli* expressing acy-ACP thioesterase from *Ricinus communis*. Metabolic Engineering. 14**,** 380-387.

Liang, X., Liao, C. Y., Thompson, M. L., Soupir, M. L., Jarboe, L. R., Dixon, P. M., 2016. *E. coli* Surface Properties Differ between Stream Water and Sediment Environments. Frontiers in Microbiology. 7.

Lowry, O. H., Rosebrough, N. J., Farr, A. L., Randall, R. J., 1951. Protein measurement with the Folin phenol reagent. Journal of Biological Chemistry. 193**,** 265-275.

Mykytczuk, N. C. S., Trevors, J. T., Leduc, L. G., Ferroni, G. D., 2007. Fluorescence polarization in studies of bacterial cytoplasmic membrane fluidity under environmental stress. Progress in Biophysics & Molecular Biology. 95**,** 60-82.

Neidhardt, F. C., Bloch, P. L., Smith, D. F., 1974. Culture medium for *Enterobacteria*. Journal of Bacteriology. 119**,** 736-747.

Rosenberg, M., Gutnick, D., Rosenberg, E., 1980. Adhyerence of bacteria to hydrocarbons - a simple method for measuring cell-surface hydrophobicity. Fems Microbiology Letters. 9**,** 29-33.

Ross, W., Sanchez-Vazquez, P., Chen, A. Y., Lee, J. H., Burgos, H. L., Gourse, R. L., 2016. ppGpp Binding to a Site at the RNAP-DksA Interface Accounts for Its Dramatic Effects on Transcription Initiation during the Stringent Response. Mol. Cell. 62**,** 811-823.

Ross, W., Vrentas, C. E., Sanchez-Vazquez, P., Gaal, T., Gourse, R. L., 2013. The Magic Spot: A ppGpp Binding Site on *E. coli* RNA Polymerase Responsible for Regulation of Transcription Initiation. Mol. Cell. 50**,** 420-429.

Roth, B. L., Poot, M., Yue, S. T., Millard, P. J., 1997. Bacterial viability and antibiotic susceptibility testing with SYTOX Green nucleic acid stain. Applied and Environmental Microbiology. 63**,** 2421-2431.

Royce, L., Boggess, E., Jin, T., Dickerson, J., Jarboe, L., 2013a. Identification of mutations in evolved bacterial genomes. Methods in molecular biology (Clifton, N.J.). 985**,** 249-67.

Royce, L. A., Liu, P., Stebbins, M. J., Hanson, B. C., Jarboe, L. R., 2013b. The damaging effects of short chain fatty acids on *Escherichia coli* membranes. Applied Microbiology and Biotechnology. 97**,** 8317-8327.

Royce, L. A., Yoon, J. M., Chen, Y., Rickenbach, E., Shanks, J. V., Jarboe, L. R., 2015. Evolution for exogenous octanoic acid tolerance improves carboxylic acid production and membrane integrity. Metabolic Engineering. 29**,** 180-188.

Sanchez-Vazquez, P., Dewey, C. N., Kitten, N., Ross, W., Gourse, R. L., 2019. Genome-wide effects on *Escherichia coli* transcription from ppGpp binding to its two sites on RNA polymerase. Proceedings of the National Academy of Sciences of the United States of America. 116**,** 8310-8319.

Santoscoy, M. C., Jarboe, L. R., 2019. Streamlined assessment of membrane permeability and its application to membrane engineering of *Escherichia coli* for octanoic acid tolerance. Journal of Industrial Microbiology & Biotechnology. in press.

Team, R. C., R: A language and environment for statistical computing (Version 3.4.1). R Foundation for Statistical Computing, Vienna, Austria, 2018.

Torella, J. P., Ford, T. J., Kim, S. N., Chen, A. M., Way, J. C., Silver, P. A., 2013. Tailored fatty acid synthesis via dynamic control of fatty acid elongation. Proceedings of the National Academy of Sciences of the United States of America. 110**,** 11290-11295.

Untergasser, A., Cutcutache, I., Koressaar, T., Ye, J., Faircloth, B. C., Remm, M., Rozen, S. G., 2012. Primer3-new capabilities and interfaces. Nucleic Acids Research. 40.

Zuo, Y. H., Wang, Y. M., Steitz, T. A., 2013. The Mechanism of *E. coli* RNA Polymerase Regulation by ppGpp Is Suggested by the Structure of their Complex. Mol. Cell. 50**,** 430-436.

Gene	Gene Mutation	Strain	Protein Mutation	Polypeptide/Enzyme	Timing of Mutation
waaG	768 bp IS removed	LAR1 LAR2	restoration of MG1655 sequence	LPS glucosyltransferase I	Between transfers #2 and #3
rpoC	A1256C	LAR1 LAR2	H419P, in very close proximity to ppGpp binding site 1, a part of the stringent response mechanism	RNA polymerase subunit β'	Complete by transfer #13
basR	G82T	LAR1	D28Y, within response regulator receiver domain	DNA-binding transcriptional dual regulator BasR	After transfer #15
basS	27 bp deletion	LAR2	Deletion of amino acids 285 – 293, within histidine kinase domain	sensory histidine kinase BasS	After transfer #15

Strain	Gene				0 mM C8		10 mM C8		20 mM C8	
	waaG^{R}	*rpoC*^{H419P}	*basR**	*basS**	Specific Growth Rate (/hr)	OD_{550} at 24 hr	Specific Growth Rate (/hr)	OD_{550} at 24 hr	Specific Growth Rate (/hr)	OD_{550} at 24 hr
LAR1	●	●	●		0.58±0.00[b]	3.01±0.04	0.58±0.00[b]	2.20±0.07[b]	0.57±0.00	1.75±0.03
ML115					0.60±0.01[a]	3.17±0.07	0.15±0.00[a]	0.29±0.01[a]		
YC001	●				0.53±0.01[a,b]	2.9±0.2	0.39±0.01[a,b]	1.57±0.03[a,b]		
YC005	●	●			0.57±0.01[a]	3.1±0.1	0.55±0.02[b]	2.20±0.02[b]	0.51±0.00[a]	1.70±0.07
YC010	●	●	●		0.57±0.00	2.98±0.04	0.57±0.01[b]	2.13±0.01[b]	0.56±0.01	1.74±0.02
YC002		●			0.65±0.01[a,b]	3.00±0.02	0.23±0.01[a,b]	0.38±0.02[a,b]		
YC003			●		0.60±0.00[a]	2.61±0.02[a.b]	0.15±0.00[a]	0.28±0.01[a]		
YC004				●	0.60±0.01	2.74±0.02[a,b]	0.16±0.00[a]	0.31±0.01[a]		
YC006	●		●		0.45±0.01[a,b]	3.0±0.1	0.35±0.01[a.b]	1.57±0.07[a,b]		
YC007	●			●	0.52±0.01[a,b]	3.0±0.1	0.35±0.01[a,b]	1.30±0.08[a,b]		
YC008		●	●		0.67±0.00[a,b]	2.88±0.05	0.16±0.00[a]	0.17±0.02[a,b]		
YC009			●	●	0.54±0.00[a,b]	2.34±0.09[a,b]	0.20±0.01[a,b]	0.21±0.01[a,b]		
YC011	●		●	●	0.47±0.01[a,b]	2.98±0.04	0.39±0.00[a,b]	1.53±0.03[a,b]		

"●" indicates that gene is present in the evolved form.

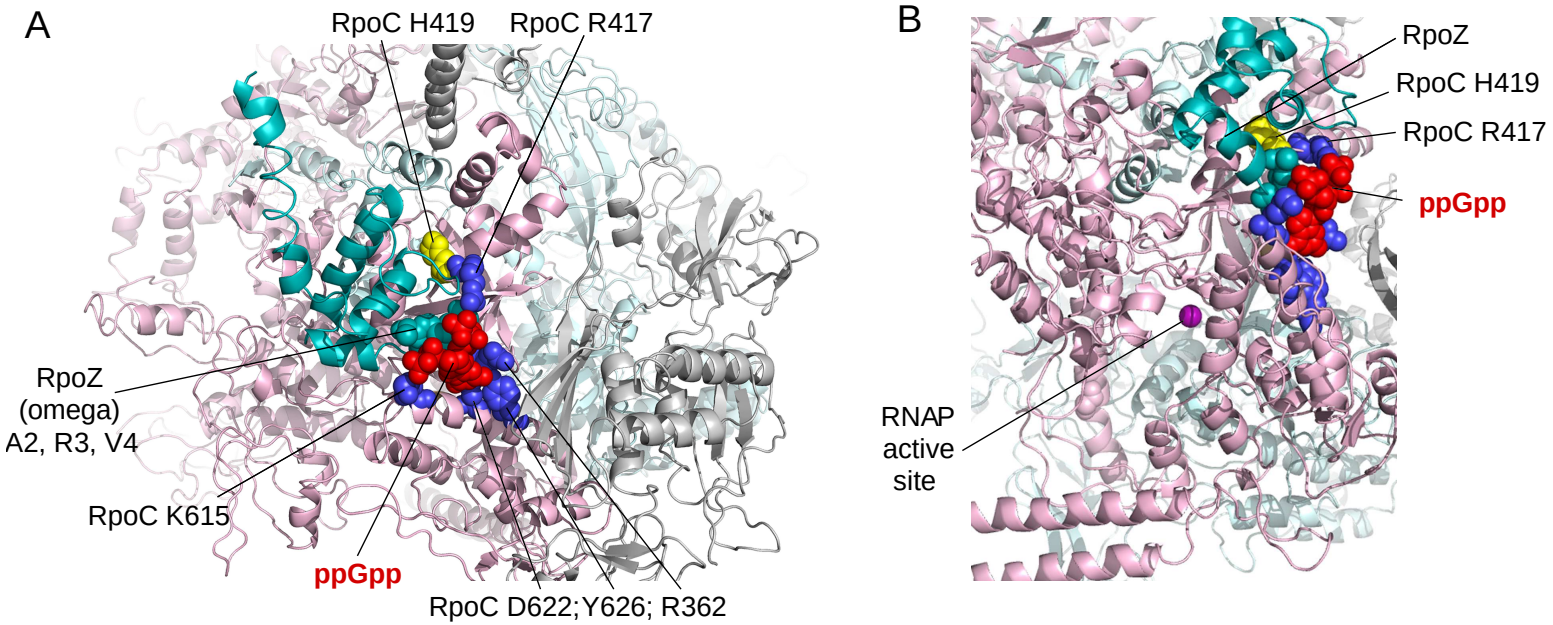
A
RpoC H419
RpoC R417
RpoZ
(omega)
A2, R3, V4
RpoC K615
ppGpp
RpoC D622;Y626; R362
B
RpoZ
RpoC H419
RpoC R417
ppGpp
RNAP
active
site

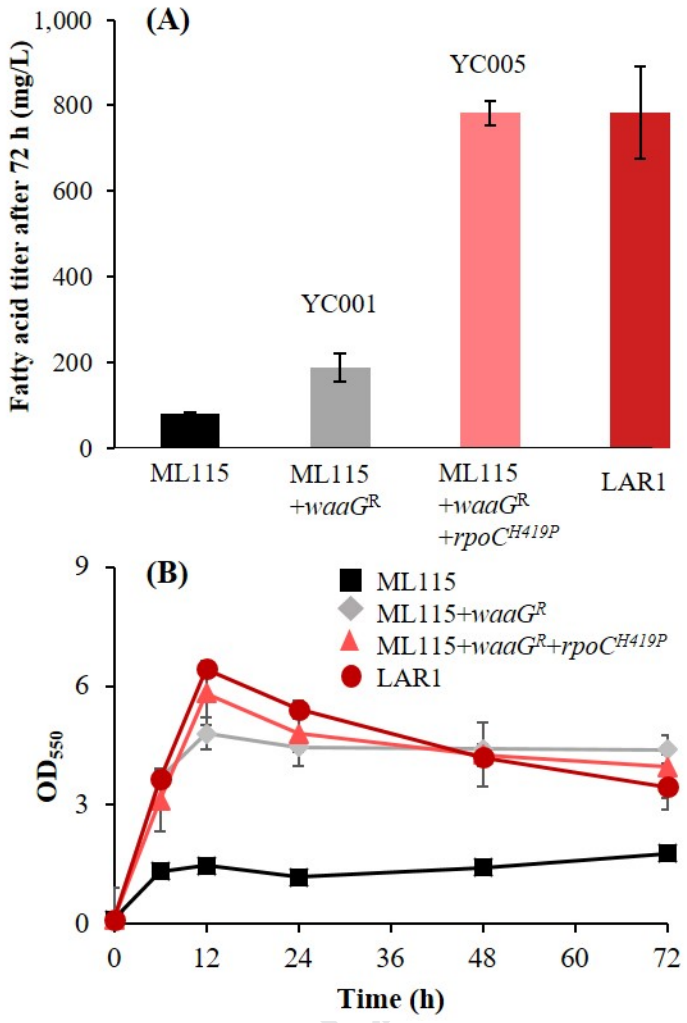

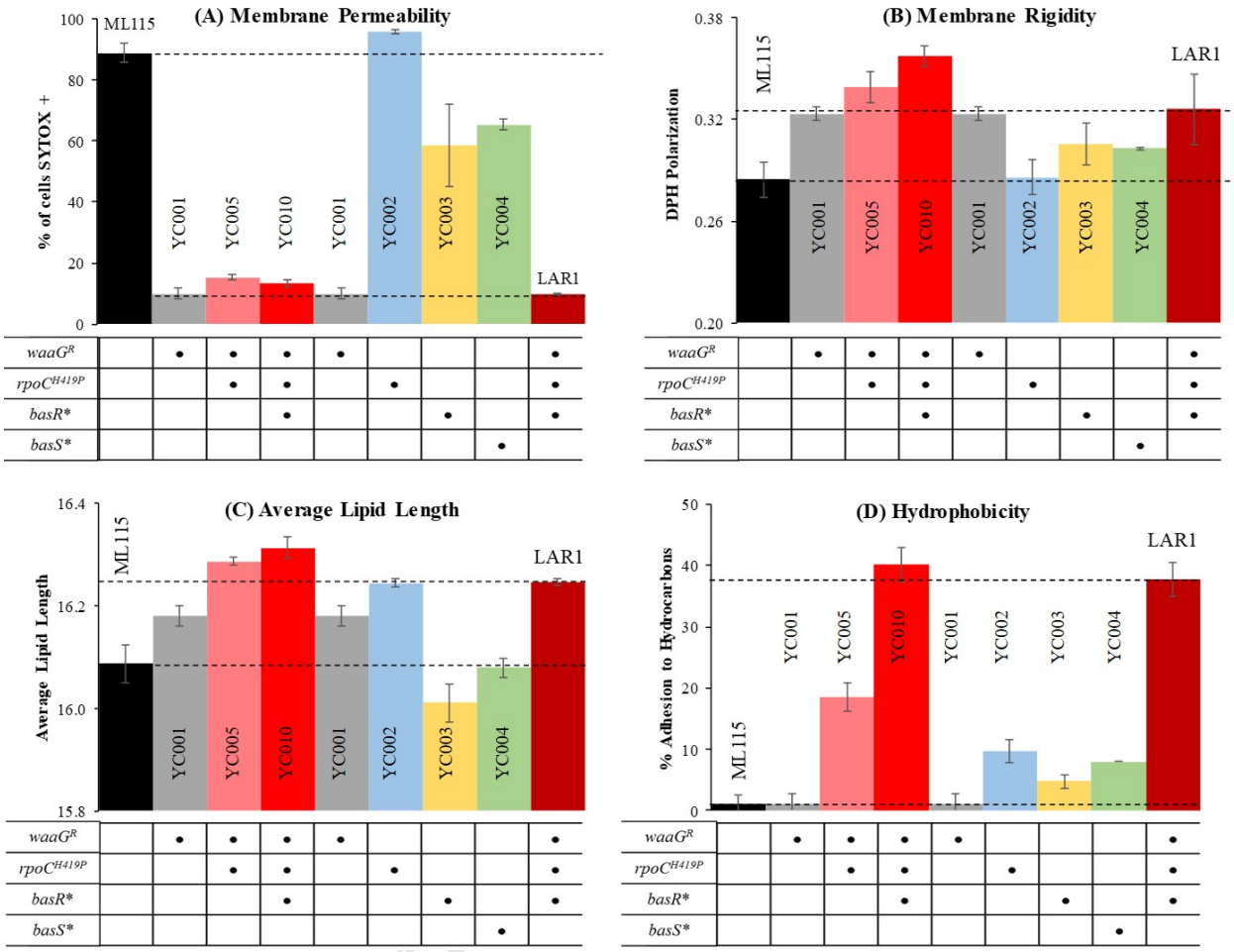
(A) Membrane Permeability
% of cells SYTOX +
100
80
60
40
20
0
ML115
YC001
YC005
YC010
YC001
YC002
YC003
YC004
LAR1
waaG^R
rpoC^H419P
basR*
basS*
(B) Membrane Rigidity
DPH Polarization
0.38
0.32
0.26
0.20
(C) Average Lipid Length
Average Lipid Length
16.4
16.2
16.0
15.8
(D) Hydrophobicity
% Adhesion to Hydrocarbons
50
40
30
20
10
0

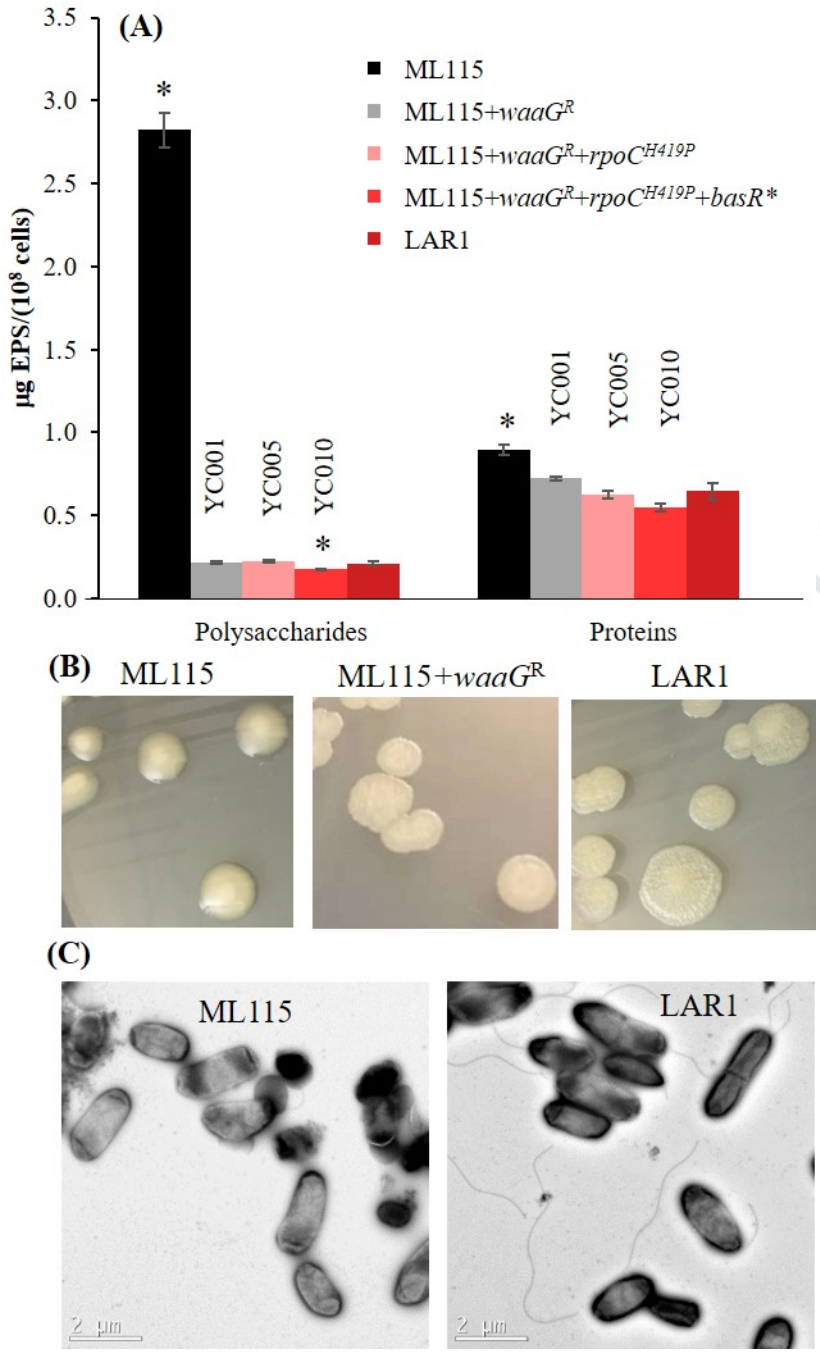
(A)
3.5
3.0
2.5
2.0
1.5
1.0
0.5
0.0
μg EPS/(10^8 cells)
ML115
ML115+waaG^R
ML115+waaG^R+rpoC^H419P
ML115+waaG^R+rpoC^H419P+basR*
LAR1
YC001
YC005
YC010
Polysaccharides
Proteins
(B)
ML115
ML115+waaG^R
LAR1
(C)
ML115
LAR1
2 μm
2 μm

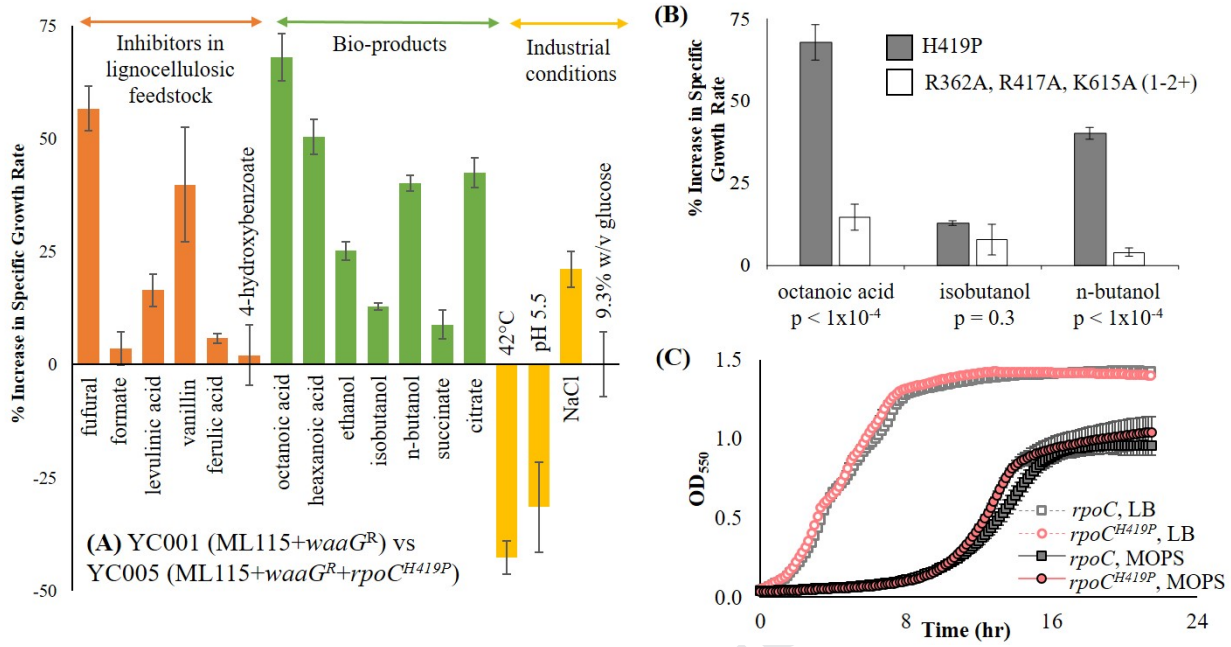

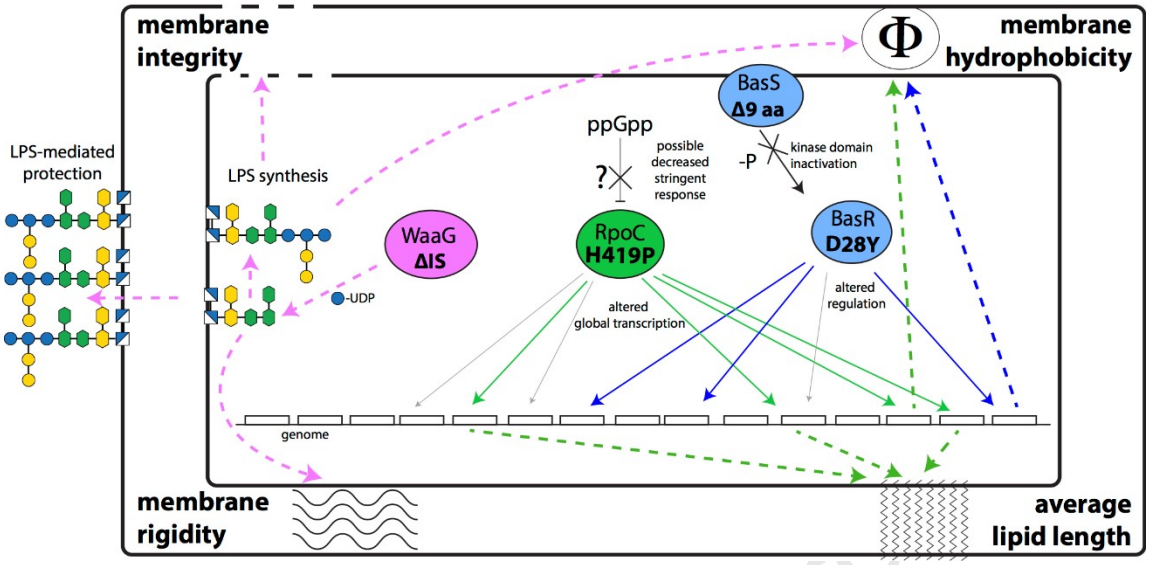

*Note: not previously peer reviewed

- RpoC H419P mutation increases fatty acid tolerance and production, lipid length
- BasS-BasR mutation improves tolerance of fatty acids at higher concentrations
- WaaG impacts EPS sugar abundance, membrane permeability and membrane rigidity
- Reverse engineering identifies timing, contribution of mutations to evolved phenotype